Modeling of spontaneous and stimulated emission of Erbium in Silicon

A thesis submitted to
the Department of Electrical and Electronic Engineering of
Bangladesh University of Engineering and Technology, Dhaka
in partial fulfillment of the requirement
for the degree of
MASTER OF SCIENCE IN ELECTRICAL AND ELECTRONIC ENGINEERING

95948
27.1.02

by

Syed Iftekhar Ali

#95948#

DEPARTMENT OF ELECTRICAL AND ELECTRONIC ENGINEERING
BANGLADESH UNIVERSITY OF ENGINEERING AND TECHNOLOGY

2002

The thesis entitled **"Modeling of spontaneous and stimulated emission of Erbium in Silicon"** submitted by Syed Iftekhar Ali, Roll No.: 040006209F, Session: April 2000 has been accepted as satisfactory in partial fulfillment of the requirement for the degree of MASTER OF SCIENCE IN ELECTRICAL AND ELECTRONIC ENGINEERING on 19/01/2002.

BOARD OF EXAMINERS

1. ______________________

Dr. Md. Quamrul Huda — **Chairman** (Supervisor)
Associate Professor
Department of Electrical and Electronic Engineering
BUET, Dhaka-1000, Bangladesh

2. ______________________

Dr. A. H. M. Zahirul Alam — **Member**
Professor
Department of Electrical and Electronic Engineering
BUET, Dhaka-1000, Bangladesh

3. ______________________

Dr. Anisul Haque — **Member**
Associate Professor
Department of Electrical and Electronic Engineering
BUET, Dhaka-1000, Bangladesh

4. ______________________

Dr. M. M. Shahidul Hassan — **Member** (Ex-officio)
Professor and Head
Department of Electrical and Electronic Engineering
BUET, Dhaka-1000, Bangladesh

5. ______________________

Dr. Md. Feroz Alam Khan — **Member** (External)
Associate Professor
Department of Physics
BUET, Dhaka-1000, Bangladesh

Declaration

It is hereby declared that this thesis or any part of it has not been submitted elsewhere for the award of any degree or diploma.

Signature of the candidate

Iftekhar
19-01-2002

(Syed Iftekhar Ali)

Dedication

To my parents

Contents

Certification of Thesis ii

Declaration iii

Dedication iv

List of Figures viii

Acknowledgement xi

Abstract xii

1 Introduction 1

1.1 Objective of the work 2

1.2 Organization of the thesis 2

2 Luminescence from Silicon 4

2.1 Direct and indirect bandgap 4

2.2 Luminescence from Silicon 5

2.2.1 Impurity enhanced luminescence from Silicon 6

2.3 Excitation mechanism of Erbium in Silicon 7

2.4 De-excitation mechanisms of Erbium in Silicon 8

2.5 Shockley-Read-Hall (SRH) generation-recombination kinetics 12

2.6 Recent work on Erbium luminescence in Silicon 13

2.7 Effect of short excitation pulse on Erbium luminescence in Silicon 15

3	**Laser Theory**		**17**
	3.1	Emission and absorption	17
	3.2	Einstein relations	18
	3.3	Absorption of radiation	20
	3.4	Optical feedback	21
	3.5	Threshold conditions	22
	3.6	Lineshape function	24
	3.7	Stimulated emission from Erbium in Silicon	25
4	**Mathematical Model for Erbium Luminescence**		**26**
	4.1	Steady-state excitation and de-excitation mechanism	26
	4.2	Time dependent rise of Erbium luminescence	30
		4.2.1 Time dependent electron occupied Erbium states	30
		4.2.2 Time dependent Erbium luminescence	31
	4.3	Decay profile of Erbium luminescence	32
	4.4	Stimulated emission from Erbium in Silicon	33
	4.5	Condition for LASER action - threshold	34
	4.6	A proposed laser device using Erbium doped Silicon	35
		4.6.1 Structure	35
		4.6.2 Formulation	37
5	**Results and Discussion**		**39**
	5.1	Parameters for Erbium incorporated Silicon	39
	5.2	Erbium luminescence as a function of excitation	43
	5.3	Erbium luminescence as a function of temperature	46
	5.4	Photoluminescence decay profile	48
	5.5	Effect of short excitation pulse on Erbium luminescence	51
	5.6	Stimulated emission and absorption	56
6	**Conclusion**		**60**
	6.1	Recommendation for future work	60

Bibliography **62**

Appendices **65**

A Flowchart for calculation of PL decay profile of Erbium in Silicon 65

B Expression of excited Erbium atoms considering Stimulated emission and absorption 66

List of Figures

2.1	E vs. k diagram for (a) direct bandgap and (b) indirect bandgap material	5
2.2	Schematic energy-level diagrams of a free Er^{3+} ion (left-hand side) and Er^{3+} in crystal field (right-hand side). Each of the free ion energy levels is split into a manifold of sublevels. (courtesy of Xie et al. [13])	7
2.3	Schematic representation of impurity Auger de-excitation processes for Er in Si : (a) Auger de-excitation with free electrons, (b) Auger de-excitation with free holes, (c) Auger de-excitation with bound electrons and (d) Auger de-excitation with bound holes.	9
2.4	Schematic representation of energy back transfer process	11
2.5	De-excitation processes of Er in Si	11
2.6	Schematic diagram of SRH generation-recombination processes : (a) electron capture, (b) electron emission, (c) hole capture and (d) hole emission.	12
2.7	Time evolution of 1.54 μm Er^{3+} luminescence during and after 30 μs excitation pulse.(courtesy of Shin et al. [17])	16
3.1	Diagram illustrating (a) stimulated absorption, (b) spontaneous emission and (c) stimulated emission. The black dot indicates the electron which takes part in the transition between the two energy levels.	18
3.2	(a) Transmission curve for transitions between two energy levels and (b) emission curve for transition between the energy levels.	24
4.1	Proposed p-n^+ junction diode laser	36
4.2	An optical cavity using the proposed diode laser	37

5.1 Calculated PL intensity profile from Erbium under variable photo-excitation. Typical values of N_{er}, N_d and T have been used. Excess carrier lifetime has been taken as 40 μs. 43

5.2 Calculated PL intensity profile under variable photo-excitation at two different temperatures. Typical values of N_{er} and N_d have been used. Excess carrier lifetime has been taken as 20 μs at 20 K and 1 μs at 130 K. 44

5.3 Calculated PL intensity profile under variable photo excitation at two different donor doping levels. $N_{er} = 10^{17}$ per cm^3 and T =40 K have been used. Excess carrier lifetime has been taken as 18.5 μs for $N_d = 10^{15}$ per cm^3 and 11.5 μs for $N_d = 4\times10^{17}$ per cm^3. 45

5.4 Calculated PL intensity profile under variable photo excitation in n-type and p-type Silicon. Typical values of N_{er} and T have been used. $N_d = N_a = 10^{17}$ per cm^3 have been used. Excess carrier lifetime has been taken as 40 μs. 46

5.5 Suggested dependence of excess carrier lifetime on temperature 47

5.6 Calculated PL dependence on temperature under constant photo-excitation using previously suggested dependence of lifetime on temperature. $N_{er}=10^{18}$ per cm^3 and $N_d=10^{16}$ per cm^3 have been used. 48

5.7 Calculated PL decay profile at two different temperatures. $N_{er} = 10^{17}$ and $N_d = 10^{16}$ per cm^3 have been used. Excess carrier lifetime has been taken as 17 μs at 40 K and 5.5 μs at 100 K. Laser power of 1mW was used for steady state excitation. Curves have been normalized to initial values. 49

5.8 Calculated luminescence decay profile at two different donor doping levels. $N_{er} = 10^{17}$ per cm^3 and T = 40 K have been used. Excess carrier lifetime has been taken as 17 μs at $N_d = 10^{16}$ per cm^3 and 12 μs at $N_d = 4\times10^{17}$ per cm^3. Laser power of 1mW was used for steady state excitation. 50

5.9 Calculated PL decay profile for n-type and p-type Silicon. $N_{er} = 10^{17}$, $N_d = N_a = 10^{16}$ per cm^3, T = 40 K and τ = 17 μs have been used. Laser power of 1mW was used for steady state excitation. 51

5.10 Calculated PL intensity, pumping rate and decay rate profile under constant photo-excitation of 25 mW. $N_{er} = 3\times10^{17}$, $N_a = 1.5\times10^{16}$ per cm^3, T = 9 K and τ = 13 μs have been used. 52

5.11 Calculated PL intensity, pumping rate and decay rate profile for 30 μs laser pulse with an excitation of 25 mW. $N_{er} = 3\times10^{17}$, $N_a = 1.5\times10^{16}$ per cm^3, T = 9 K and τ = 13 μs have been used. 53

5.12 Calculated PL intensity profile under 30 μs laser pulse excitation of 100 mW. $N_{er} = 3\times10^{17}$, $N_a = 1.5\times10^{16}$ per cm^3, T = 9 K and τ = 13 μs have been used. Excellent match with experimental data extracted from Shin et al. [17] has been found. 54

5.13 Calculated PL intensity profile under 30 μs laser pulse excitation of 1 mW at two different temperatures. $N_{er} = 10^{17}$, $N_d = 4\times10^{17}$ per cm^3 have been used. τ = 40 μs at T = 9 K and τ = 11.5 μs at T = 40 K. Both the curves have been normalized to peak values. 55

5.14 Calculated PL intensity profile under 30 μs laser pulse excitation at two different excitation levels. $N_{er} = 10^{17}$, $N_d = 4\times10^{17}$ per cm^3, T = 9 K, τ = 40 μs have been used. Both the curves have been normalized to peak values. 56

5.15 Variation of N_2-N_1 with excess carriers with stimulated emission and absorption taken into consideration. $N_{er} = 10^{18}$, $N_a = 4\times10^{16}$ per cm^3, T = 4.2 K, τ = 5.8 μs have been used. 57

5.16 Calculated output power dependence of semiconductor laser on injected current density. $N_{er} = 10^{18}$, $N_a = 4\times10^{16}$ per cm^3, T = 4.2 K, τ = 5.8 μs have been used. 59

Acknowledgement

It is the utmost pleasure of the author to express sincere appreciation and heartiest gratitude to his thesis supervisor, Dr. Md. Quamrul Huda, Associate Professor, Department of Electrical and Electronic Engineering, Bangladesh University of Engineering and Technology, Dhaka, Bangladesh for his excellent supervision, valuable suggestions and continuous inspiration throughout the progress of the work. Without his whole-hearted supervision, this work would not have been possible.

The author is grateful to Dr. M. M. Shahidul Hassan, Professor and Head, Department of Electrical and Electronic Engineering, Bangladesh University of Engineering and Technology, Dhaka, Bangladesh for his kind help and cooperation.

Sincere thanks to friends for their encouragement and cooperation. Especially the encouraging words from Mr. K. Alam, Mr. Md. Yunus, Mr. S. Asaduzzaman and Mr. T. M. Islam are highly appreciated.

The author would like to thank his parents for their inspiration and patience, which made this thesis come to a fruitful end.

The author is obliged to all officers and staff of the Department of Electrical and Electronic Engineering, BUET, for their cooperation throughout the work.

Finally, the author recalls with gratitude the contributions of all the individuals involved somehow in the completion of this work.

Abstract

An improved mathematical model for the Erbium excitation and de-excitation process in both p-type and n-type Silicon at room temperature and at higher excitation conditions has been developed. Shockley-Read-Hall (SRH) recombination kinetics has been used as the basis of energy transfer to Erbium atoms in Silicon. Erbium atoms have been considered as impurity centers in Silicon. The corresponding defect level in the band gap has been assigned with values of thermal emission and capture coefficients for charge carriers. Capture and emission rates of carriers in Erbium related levels have been equated. Both spontaneous emission and stimulated emission have been studied. A number of rate equations have been solved numerically or analytically. Dependency of steady state and time dependent luminescence on temperature, excitation power, background doping, Erbium doping etc. has been analyzed with the help of the solutions. Results obtained from the calculation have been compared to published experimental data and excellent agreement has been found.

The possibility of obtaining laser from Er-doped Silicon has been investigated. For this purpose, a two level laser model has been used where electron-hole recombination through Erbium sites has been considered as the pumping source. Conditions for population inversion and threshold condition have been studied. It has been found that there is a possibility of obtaining laser from Er doped p-type Si. Finally an optical cavity has been suggested for possible laser operation and its feasibility has been studied theoretically.

Chapter 1

Introduction

Silicon is the leading semiconductor in today's microelectronic industry. Due to mature processing technology and continuous improvement in scale integration, this semiconductor is able to satisfy the increasing demand for higher complexity integrated circuits. There is no doubt that Silicon technology will dominate the semiconductor market for at least a few more decades. The demand for increased speed and compactness in integrated circuits is generating considerable interest in the development of Silicon-based optoelectronic devices and systems for interchip and intrachip communications. Unfortunately, due to its indirect bandgap nature, Silicon cannot be directly used as an efficient light emitter. Considerable efforts have been made in recent years to develop a Silicon based light source.

The issue of Silicon light source is still at an early stage and several different approaches have been tried to circumvent the problem. Among these, introduction of the rare earth element Erbium in Silicon has so far been the most promising technique. Er-doped Silicon (EDS) exhibits a sharp luminescence at 1.54 μm due to the internal 4f-shell transition ($^4I_{13/2}$ – $^4I_{15/2}$) of Erbium atoms. This 1.54 μm luminescence is of particular interest to telecommunication engineers as losses in optical fiber are minimum at this wavelength.

Despite the promising result, this field remained unexplored due to the lack of room temperature photoluminescence and electroluminescence at early stages of research. But recently the observation of photoluminescence [1] and electroluminescence [2] at room temperature has grown new interest in EDS. Thus rare earth element Erbium

may play an important role in development of complex Si based optoelectronic integrated circuits capable of operating at GHz frequency level.

1.1 Objective of the work

While it is clear that Er atoms take the recombination energy of electron-hole pairs to reach first excited state ($^4I_{13/2}$), there is a dispute over the process of this energy transfer. Different authors have proposed different theories and a number of excitation models have been developed so far. The objective of this research is to improve an existing model [3] for the Erbium excitation and de-excitation process in Silicon. Shockley-Read-Hall (SRH) recombination kinetics will be used as the basis of energy transfer to Erbium atoms. Spontaneous and stimulated emission from Erbium under different temperature and excitation conditions will be studied. Parameters such as background doping, Erbium concentration, processing conditions etc. will be considered in the model. Room temperature conditions will be included by the concept of energy back transfer from Erbium atoms. High excitation conditions, as needed for stimulated emission will be incorporated in the model by the inclusion of Auger de-excitation process. Rate equations regarding stimulated emission will be analyzed for conditions of population inversion and optical amplification. Finally a laser device will be proposed and its suitability for possible laser application will be analyzed.

1.2 Organization of the thesis

We know that due to indirect bandgap structure Silicon is incapable producing light. Chapter one of this thesis describes the necessity of developing Silicon based optoelectronic devices.

Chapter two deals with band structure of Si, optical property of Erbium, different approaches for obtaining light from Si, excitation mechanisms of Er in Si as proposed by different authors, de-excitation mechanism of Er, Shockley-Read-Hall

recombination kinetics, literature review and effect of short excitation pulse on time varying luminescence profile.

In chapter three the preliminary concepts of laser will be discussed to aid the understanding of stimulated excitation and de-excitation mechanism.

Mathematical model for excitation and de-excitation of Er in Si will be developed in chapter four. The model will include analysis of steady state and time varying spontaneous excitation and de-excitation mechanisms as well as steady state stimulated excitation and de-excitation mechanisms. Also a laser device will be proposed in this chapter.

Chapter five discusses the results obtained from the analysis. Some suggestions will be made regarding possible application of EDS in high-speed optoelectronics. Also the feasibility of the proposed laser device will be analyzed.

Chapter six discusses the conclusion on the results and recommendation for future work.

Chapter 2

Luminescence from Silicon

In this chapter we shall discuss preliminary theory of the luminescence mechanism of Er doped Si. Discussion of excitation and de-excitation mechanisms of Er atoms in Si as well as literature review will be carried out. Shockley-Read-Hall recombination kinetics, which is the basis of the excitation mechanism used in our model, will be discussed. The chapter ends with the discussion of effect of short excitation pulse on Er luminescence the explanation of which is provided in chapter five.

2.1 Direct and indirect bandgap

The band structure, i.e., the energy vs. propagation constant curve (E-k) of crystalline solid can be classified into two categories depending on the values of propagation constant at conduction band minimum and valence band maximum. In Figure 2.1 (a) these two values are equal. This kind of bandgap structure is called *direct bandgap.* GaAs, $Al_xGa_{1-x}As$ etc. are some materials having direct bandgap structure and these are called direct bandgap material. In Figure 2.1 (b) the values of k at conduction band minimum and valence band maximum are not same. This kind of bandgap structure is called *indirect bandgap.* Materials such as Si, Ge, $Si_{1-x}Ge_x$ have indirect bandgap and are called indirect bandgap material.

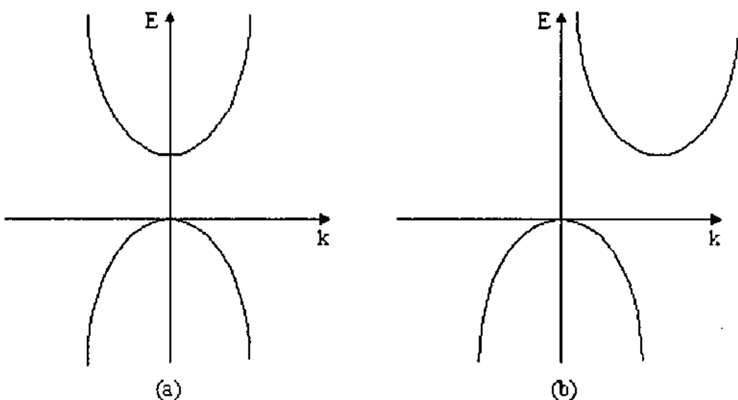

FIG. 2.1 E vs. k diagram for (a) direct bandgap and (b) indirect bandgap material

In direct bandgap materials electrons can make a smallest-energy transition from conduction band to an empty state in valence band without any change in propagation constant. The recombination energy is given up in form of photons having energy corresponding to the bandgap energy. This kind of recombination process is called *radiative recombination.*

In indirect bandgap materials the recombination can not occur directly but through a recombination level within the bandgap or via involvement of a third particle like a charge carrier or phonon. The electron must undergo a change in propagation constant as well as momentum and energy for the transition and the recombination energy is generally given up as heat which is dissipated in the crystal lattice. This process is called *non-radiative recombination.* The indirect bandgap structure in Si is responsible for inefficient light emission from Si. The recombination level via which the transition can take place may be introduced by impurity doping or by lattice defect.

2.2 Luminescence from Silicon

Different approaches have been tried to circumvent the problem of physical inability of Silicon to produce light. Among these use of porous Si [4], Si-rich Silicon oxide [5], $Si_{1-x}Ge_x$ heteroepitaxy on Silicon [6] and introduction of impurity levels are worth mentioning. Impurity luminescence can be further divided into luminescence

through isovalent centers [7] and luminescence through rare earth (RE) impurities [8,9,10]. In particular introduction of rare earth elements, specifically Erbium in Si has emerged as a quite promising route towards Si-based optoelectronics.

2.2.1 Impurity enhanced luminescence from Silicon

An isovalent impurity is an impurity which has same outer electronic structure as the host material. But the electronic core structure is different. Carbon, Germanium, Tin etc. are examples of isovalent impurities in Si. These atoms introduce trap levels in Si that are used as recombination centers.

The most important characteristic of luminescence in RE elements is the optical transitions involved between the internal energy levels of the RE ions which is responsible for the emission of photons. It is well established now [11] that RE elements have a strong tendency of being in a 3+ valence electronic state when incorporated in alloys or doped as impurities in a host material. The observed transitions from the RE^{3+} ions are internal transitions of the 4f states [12]. These transitions are forbidden in case of free ions by the parity selection rule, but are made possible by the crystal field in the case of RE^{3+} ions in solid. The crystal field intermixes states of opposite parities and splits each single state of a free RE^{3+} ion into a manifold of substates with slightly different energies (Figure 2.2).

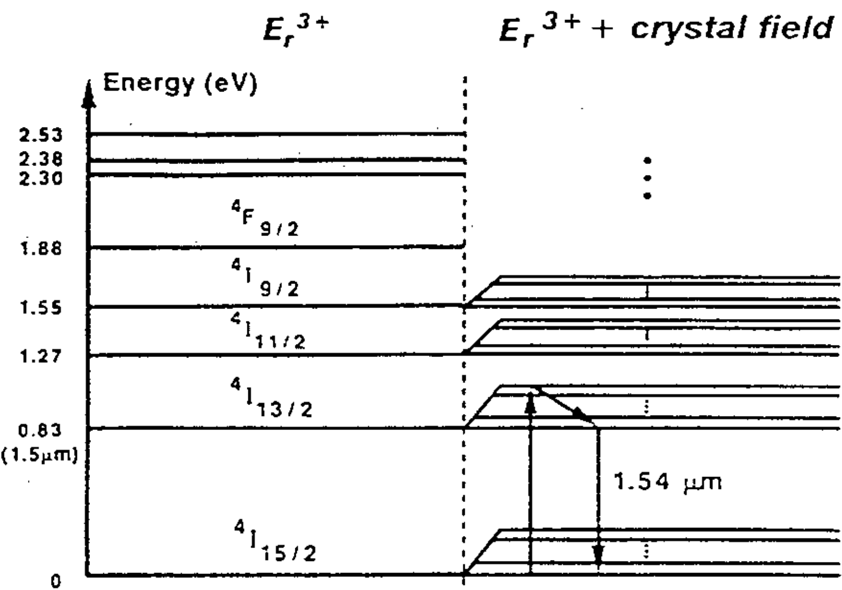

FIG. 2.2 Schematic energy-level diagrams of a free Er^{3+} ion (left-hand side) and Er^{3+} in crystal field (right-hand side). Each of the free ion energy levels is split into a manifold of sublevels. (courtesy of Xie et al. [13])

The degree of parity mixing is, in general, small. As a result the transition probability is also small which in turn results in a long spontaneous emission lifetime τ_{rad}. The luminescence properties are independent on the host materials due to the fact that the 4f electrons are well shielded by the outer 5s, 5p, ... electrons. This is evidenced by the fact that $\tau_{rad} \approx 1$ms and $\lambda \approx 1.54\ \mu$m for Er-doped GaP, InP, GaAs and Si.

2.3 Excitation mechanism of Erbium in Silicon

Whenever Si is doped with an impurity, a trap level is formed in Silicon bandgap. It has been shown [14,15,16,17] that in the presence of O, Er introduces a trap level at around 0.15 eV below the Si conduction band which is involved in Er excitation. The actual mechanism of Er luminescence is yet to be understood. It is now well established that energy given up by e-h recombination is the source of Er excitation. But there are disputes over the process how the recombination takes place. Different authors have proposed different mechanisms. It has been suggested that the

excitation mechanism involves electron-hole complexes through sequential capture of electrons and holes at an Erbium related levels [16,18]. Electron-hole pairs can form bound states called excitons due to coulomb attraction between them. Excitons can be attracted by impurity atoms and can form bound excitons in extrinsic semiconductors. After excess carrier generation, formation of excitons bound to Er atoms and energy given up by their subsequent recombination is said to be the source of Er excitation by Palm et al. [19]. The same excitation mechanism has also been suggested by Shin et al. [17] and Coffa et al. [20]. Recently Huda et al. [3] has proposed an excitation model based on Shockley-Read-Hall recombination kinetics. They pointed out that after the generation of excess carriers by electrical or optical excitation, electrons from conduction band recombine with holes in valence band via Er related levels within the Si bandgap. The recombination energy excites Er atoms from ground state ($^4I_{15/2}$) to the first excited state ($^4I_{13/2}$). Radiative transition of excited Er atoms causes emission of photons. The rate of excitation is controlled by the emission and capture rates of electrons and holes by Er related levels. The model however is applicable only for low temperature and low excitation operation.

2.4 De-excitation mechanisms of Erbium in Silicon

There are two possible de-excitation processes of excited Er atoms in Si. The first one is radiative de-excitation with a lifetime of approximately 1 ms [13]. This de-excitation process in responsible for photon emission. The second one is non-radiative de-excitation process which does not produce useful light output. Here, instead of emitting photons, the energy given up by the transition from excited state ($^4I_{13/2}$) to ground state ($^4I_{15/2}$) is wasted. The wastage can occur in two different ways. Depending on the way of de-excitation, non-radiative de-excitation of Er in Si has been categorized into two different classes such as (i) *impurity Auger de-excitation* and (ii) *energy back transfer*.

(i) Impurity Auger de-excitation : In impurity Auger de-excitation process the energy given up by relaxation of Er atoms is delivered to free carriers (electrons in conduction band or holes in valence band) or carriers bound to shallow donor or

acceptor level. By absorbing the energy, free carriers and/or bound carriers go to higher energy states. According to the recipient of the energy, the impurity Auger process can be further classified into two : (a) *Auger de-excitation with free carriers* and (b) *Auger de-excitation with bound carriers.* Figure 2.3 demonstrates various impurity Auger de-excitation processes.

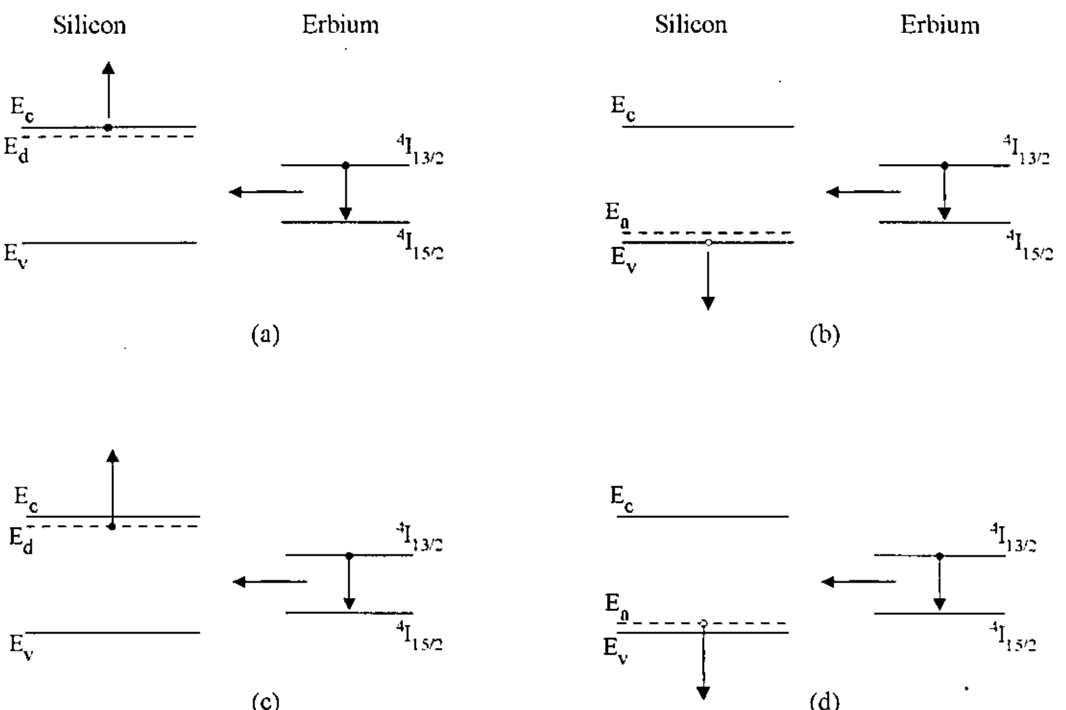

FIG. 2.3 Schematic representation of impurity Auger de-excitation processes for Er in Si : (a) Auger de-excitation with free electrons, (b) Auger de-excitation with free holes, (c) Auger de-excitation with bound electrons and (d) Auger de-excitation with bound holes.

The formulation of these effects has been done by Priolo et al. [16] and is as follows

(a) *Impurity Auger de-excitation with free carriers* : The probability of occurrence of this process has been found to be directly proportional to the number of free carriers present. So a lifetime corresponding to this process can be defined as inversely proportional to the number of free carriers. The free carriers may be generated by optical excitation or electrical injection as well as by thermal dissociation of carriers from shallow donor or acceptor level. Priolo et al. [16] has proposed that this effect can be expressed mathematically by

$$\frac{1}{\tau_{Af}} = C_{Ae}n \quad \text{for n-type Si}$$

$$\text{and} \quad \frac{1}{\tau_{Af}} = C_{Ah}p \quad \text{for p-type Si}$$

where C_{Ae} and C_{Ah} are called Auger coefficient for free carriers, n and p are the free electron and hole concentrations respectively.

(b) *Impurity Auger de-excitation with bound carriers* : In this case also the probability of occurrence is directly proportional to the number of carriers bound to shallow donor or acceptor level. So, as before this effect can be expressed mathematically by

$$\frac{1}{\tau_{Ab}} = C_{Abe}n_b \quad \text{for n-type Si}$$

$$\text{and} \quad \frac{1}{\tau_{Ab}} = C_{Abh}p_b \quad \text{for p-type Si}$$

where C_{Abe} and C_{Abh} are Auger coefficients for bound carriers, and n_b and p_b are concentration of carriers bound to donor and acceptor levels respectively.

It has been found [16,19] that impurity Auger de-excitation process can nicely describe the temperature quenching effect in low temperature range, i.e., upto 150° K at which most of the shallow levels are ionized. So at 150° K the process reaches saturation. Above this temperature another mechanism must be in effect in the process of temperature quenching. This process is the energy back transfer process.

(ii) **Energy back transfer** : As mentioned in section 2.3, Er atoms are excited when electrons trapped in Er related level recombine with holes in valence band. The reverse process is also possible. In this process, the energy given up by relaxation of Er atoms excites electrons from valence band to Er level. This process is exactly the reverse of excitation and hence has been named energy back transfer as energy is transferred back through the same path. The energy given up by relaxation of Er atoms is not sufficient for the transition and the extra energy ΔE needed for this is supplied by phonons. Figure 2.4 illustrates energy back transfer mechanism.

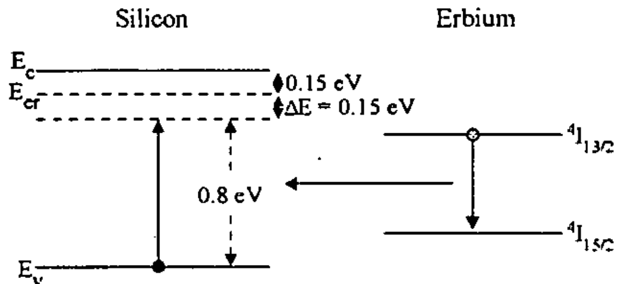

FIG. 2.4 Schematic representation of energy back transfer process.

As phonons are involved in this process, this process is expected to be thermally activated. The energy back transfer process is characterized by an activation energy of 0.15 eV and hence must always be completed by thermalization of electron trapped at Er-related level to the conduction band [16]. Both Priolo et al. [16] and Kik et al. [21] have mathematically expressed this process by defining a lifetime related to energy back transfer process as follows

$$\frac{1}{\tau_{bt}} = W_0 \exp\left(-\frac{0.15\,\text{eV}}{kT}\right)$$

where W_0 is a fitting parameter (in s^{-1}) , k is Boltzmann's constant (in eV/K) and T is absolute temperature (in °K). Energy back transfer can successfully explain the high temperature quenching phenomenon of Er luminescence in Si.

So from above discussion different de-excitation processes of Er in Si can be categorized as shown in Figure 2.5

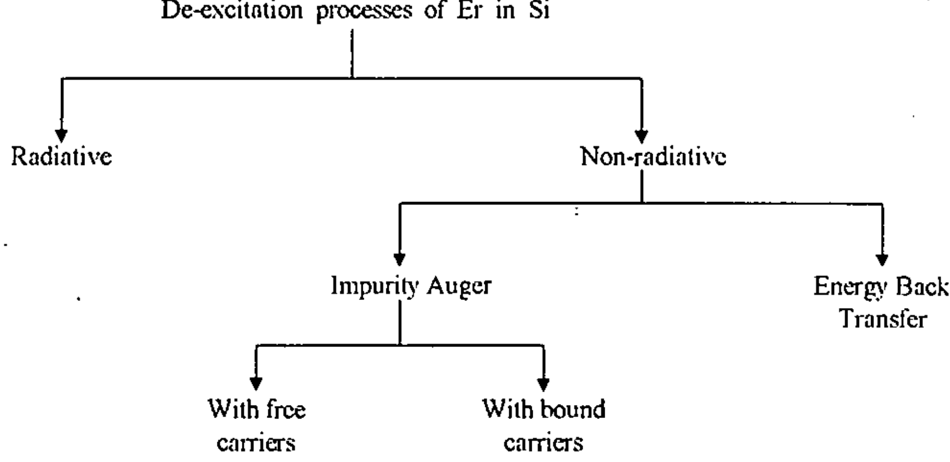

FIG. 2.5 De-excitation processes of Er in Si

2.5 Shockley-Read-Hall (SRH) generation -recombination kinetics

According to Shockley-Read-Hall recombination kinetics, there are basically four processes involving generation-recombination of electron-hole pairs [22]. These processes are as follows :

(i) **Electron capture** : The rate of electron capture by a trap level is proportional to number of electrons available for capture and number of empty trap centers. If the concentration of traps per unit volume is N_t, then the recombination rate for electrons is given by

$$R_n = c_n n N_t (1 - f_t)$$

where c_n is the capture coefficient for electrons, n is the free electron concentration and f_t is the occupation probability of the trap.

(ii) **Electron emission** : The rate of electron emission from the trap level into the conduction band is proportional to the number of electron occupied traps. Thus the rate of free electron generation is given by

$$G_n = e_n N_t f_t$$

where e_n is the electron emission rate.

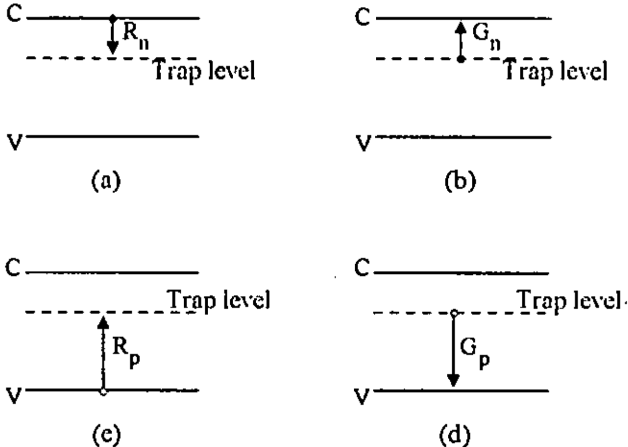

FIG. 2.6 Schematic diagram of SRH generation-recombination processes : (a) electron capture, (b) electron emission, (c) hole capture and (d) hole emission.

(iii) **Hole capture** : The rate of recombination of holes at a trap level is proportional to number of holes available and number of electron occupied trap centers. So the rate is given by

$$R_p = c_p p N_t f_t$$

where c_p is the capture coefficient for holes.

(iv) **Hole emission** : The generation rate of holes due to this process is proportional to the number of empty trap sites. So

$$G_p = e_p N_t (1 - f_t)$$

where e_p is the hole emission rate.

At thermal equilibrium net generation-recombination of electrons and holes is zero. So

$$R_n - G_n = R_p - G_p = 0$$

2.6 Recent work on Erbium luminescence in Silicon

Luminescence from Er doped Si was first observed by Ennen et al. [8]. Since then extensive work has been done in this field. Ennen et al. [23] and Tang et al. [24] carried out photo emission analysis from Er in Si. They demonstrated that most of the optically active Er^{3+} ions have tetrahedral or lower site symmetries on interstitial lattice sites in Si. Enhancement of luminescence in the presence of impurities such as O, C, N, F or Br has been found by a number of authors. Michel et al. [1] found a large enhancement of luminescence intensity by introducing Oxygen. By using Extended X-ray Absorption Fine Spectroscopy (EXAFS) analysis, Alder et al. [25] found that the impurities modify the chemical surrounding of Er in Si and form Er:impurity complex. Since O activates Er optically, researchers are very much interested in Si:Er system with O co-dopant.

Er has demonstrated to present donor behavior in Si [26]. It was pointed out that Oxygen co-implant enhances Er donor activity [14,27]. They suggested that this

donor behavior might be the result of the formation of Er - O complexes in EDS. Based on these results Priolo et al. [27] suggested that electrical and optical activation of Er in Si could be correlated, i.e., the Er donor behavior might be associated with the Er^{3+} state. Coffa et al. [20] also showed that incorporation of Oxygen increases the electrical and optical activation of Er in Si.

Sharp fall of luminescence intensity with increasing temperature is the major limitation of Si:Er luminescence. This phenomenon is called *temperature quenching*. Coffa et al. [28] demonstrated the temperature dependence of 4f shell intensity by arguing that elevated temperature causes ionization of optically active Er sites and reduction of the number of excitable Er centers. They found that time-decay curves showed a fast initial decay followed by a slow decay. Priolo et al. [15] suggested that the thermalization of bound electrons to the conduction band is the cause of temperature quenching. Kik et al. [21] performed luminescence decay measurement within the temperature range 12° - 170° K. They observed that the luminescence intensity decreases by three orders of magnitude as temperature rises from 12° to 150° K. They pointed out that dissociation of bound excitons and non-radiative energy back transfer process are responsible for temperature quenching. Priolo et al. [16] has made an extensive study on the de-excitation mechanism of Er in Si. They and Palm et al. [19] proposed that non-radiative energy back transfer process is the cause of temperature quenching.

Priolo et al. [15] and Coffa et al. [28] demonstrated that co-doping with impurities such as O, C or F reduced temperature quenching significantly. Franzò et al. [2] tried to achieve room temperature electroluminescence from Er and O co-doped crystalline p-n Si diodes under both forward and reverse biased conditions. They suggested that Er excitation occur through electron-hole mediated processes under forward biased condition and through impact excitation under reverse biased condition. They found that temperature quenching could be significantly reduced while operating under reverse biased condition. Using different voltage pulse schemes for forward bias and reverse bias conditions, Palm et al. [19] analyzed the decay profile of electroluminescence. They found that under reverse bias condition,

luminescence decayed more slowly than the forward bias case. From this, they concluded that non-radiative impurity Auger process is dependent on availability of free carriers. Franzò et al. [29] and Coffa et al. [30] have shown that efficient and fast modulating LED's can be fabricated when exciting the Er ions within the depletion region of a reverse biased p^+-n^+ junction. During operation the Auger quenching is inhibited within the depletion region due to absence of free carriers but it suddenly sets in when, at the diode turn off, the depletion region shrinks [16]. Frequencies in the range of 80 MHz are achievable in these LED's [29]. So far very little work has been done on possible achievement of LASER from Er doped Si. Prospect of population inversion and light amplification has been studied by Xie et al. [13] and it has been shown theoretically that it is possible to obtain LASER if extremely efficient pumping mechanism can be used.

2.7 Effect of short excitation pulse on Erbium luminescence in Silicon

Shin et al. [17] observed an interesting phenomenon when laser pulse of short duration was used for excitation. They noticed that for an excitation pulse of 30 μs the PL intensity continues to rise even ~50 μs after the termination of the pulse. The time evolution of 1.54 μm Er^{3+} luminescence at 9° K during and after the excitation pulse is shown in Figure 2.7.

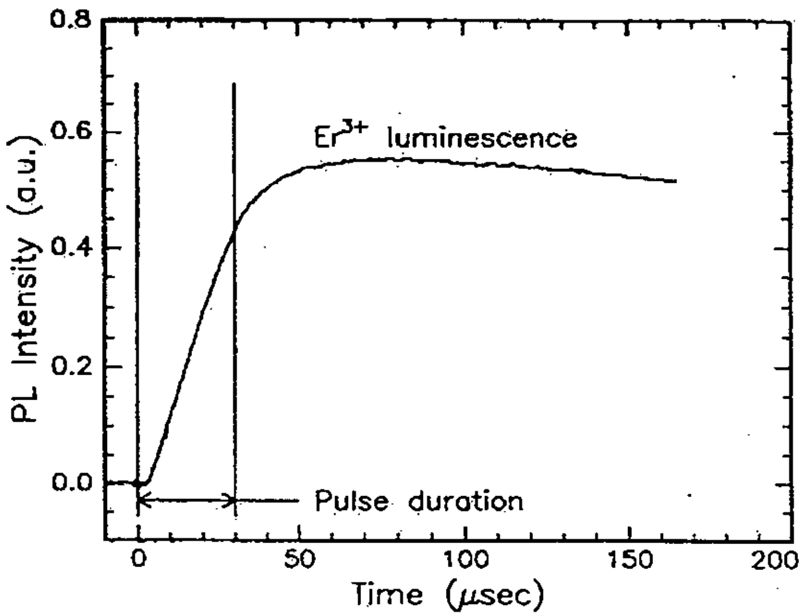

FIG. 2.7 Time evolution of 1.54 μm Er^{3+} luminescence during and after 30 μs excitation pulse.(courtesy of Shin et al. [17])

They demonstrated that Er^{3+} ions were still being excited at an appreciable rate even 50 μs after the excitation pulse is switched off. From this phenomenon, they concluded that Er^{3+} ions in Si are excited by recombination of carriers trapped at a state in the forbidden gap of Si and supported the possibility of involvement of bound excitons in the excitation process. But they could not give any explanation of the phenomenon. Recently Huda et al. [3] has provided an explanation of this. Though their model is applicable to only low temperature and low excitation conditions, they are able to show the extended rise of luminescence mathematically. In our research also we are able to explain the same thing with the help of our model.

Chapter 3

Laser Theory

The word LASER is the abbreviation of "Light Amplification by Stimulated Emission of Radiation". So the keywords in the discussion of laser theory are stimulated emission and light amplification. In this chapter the concept of stimulated emission, conditions for light amplification and supporting theory will be discussed in a simplified form.

3.1 Emission and absorption

The transition of an electron between two energy states is always accompanied by emission or absorption of a photon. The frequency of emitted or absorbed photon is described by $\nu = \Delta E/h$ where ν is the frequency and ΔE is the energy difference between two levels concerned. If there is an electron in lower energy level E_1 then it may be excited to upper level E_2 by absorbing a photon of energy $\Delta E = E_2 - E_1$ provided the photon is available. Conversely an electron in upper level may return to lower level by emitting a photon of energy ΔE. There are two ways by which the emission can take place. In *spontaneous emission* process the electron drops to lower level in an entirely random fashion. In *stimulated emission* process the transition is initiated by the presence of a photon of right frequency. Figure 3.1 illustrates the absorption and emission processes.

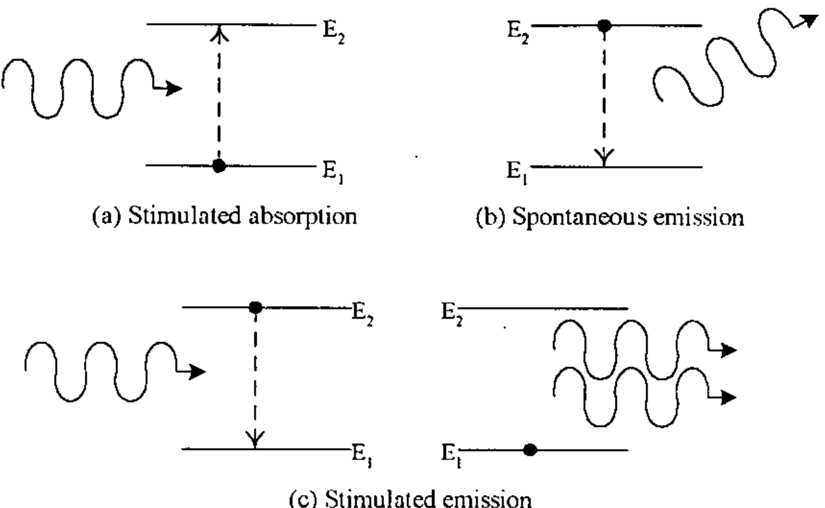

FIG. 3.1 Diagram illustrating (a) stimulated absorption, (b) spontaneous emission and (c) stimulated emission. The black dot indicates the electron which takes part in the transition between the two energy levels.

Normally the probability of occurrence of spontaneous process is much higher than that of stimulated process. As the spontaneous emission occurs randomly, radiation emitted by large number of atoms by this process is incoherent. But the stimulated emission process results in coherent radiation since the stimulating and stimulated photons have same frequency and same state of polarization and are unidirectional and are in phase. So the amplitude of an incident wave can increase by stimulated emission as it passes through a collection of excited atoms. This is obviously an amplification process of the light wave. The absorption process as the stimulated emission process can occur only in the presence of photons of appropriate energy and hence it is often referred to as *stimulated absorption*.

3.2 Einstein relations

If there are N_1 atoms per unit volume in the collection with energy E_1, then the upward transition rate or absorption rate is proportional to both N_1 and the number of photons of correct frequency, i.e., power density. So absorption rate = $N_1 \rho_\nu B_{12}$ where B_{12} is a constant and ρ_ν is power density which is given by $\rho_\nu = Nh\nu$. Here N is number of photons per unit volume having frequency ν. Similarly if there are N_2

atoms per unit volume in the collection with energy E_2, the stimulated emission rate is given by $N_2\rho_\nu B_{21}$ where B_{21} is a constant. The spontaneous emission rate is simply N_2/τ_{21} where τ_{21} is the spontaneous lifetime. So the total downward transition rate = $N_2\rho_\nu B_{21} + N_2/\tau_{21}$. According to Einstein, for a system in thermal equilibrium the rate of upward transition must be equal to the rate of downward transition. So

$$N_1\rho_\nu B_{12} = N_2\rho_\nu B_{21} + N_2/\tau_{21} \quad (3.2.1)$$

or

$$\rho_\nu = \frac{1/(\tau_{21}B_{21})}{\frac{B_{12}}{B_{21}}\frac{N_1}{N_2} - 1} \quad (3.2.2).$$

The populations of various energy levels of a system in thermal equilibrium are given by Boltzmann statistics to be

$$N_j = \frac{g_j N_0 \exp(-E_j/kT)}{\Sigma g_i \exp(-E_i/kT)} \quad (3.2.3)$$

where N_j is the population density of the energy level E_j , N_0 is the total population density, and g_j is the degeneracy of the jth level. So

$$\frac{N_1}{N_2} = \frac{g_1}{g_2}\exp((E_2 - E_1)/kT) \quad (3.2.4).$$

Therefore substituting equation (3.2.4) in equation (3.2.2)

$$\rho_\nu = \frac{1/(\tau_{21}B_{21})}{\frac{B_{12}}{B_{21}}\frac{g_1}{g_2}\exp(h\nu/kT) - 1} \quad (3.2.5).$$

Since the collection of atoms in the system is in thermal equilibrium it must give rise to radiation which is identical to blackbody radiation. So the radiation density can be described by

$$\rho_\nu = \frac{8\pi h\nu^3}{c^3}\frac{1}{\exp(h\nu/kT) - 1} \quad (3.2.6).$$

Comparing equations (3.2.5) and (3.2.6) we get

$$g_1 B_{12} = g_2 B_{21} \quad (3.2.7)$$

and $$\frac{1/\tau_{21}}{B_{21}} = \frac{8\pi h\nu^3}{c^3} \qquad (3.2.8).$$

Equations (3.2.7) and (3.2.8) are called *Einstein relations*. The ratio g_1/g_2 is generally in the order of unity and hence ignored. Thus taking refractive index of the medium into account we get

$$B_{12} = B_{21} = \frac{c^3}{8\pi h\tau_{21}\nu^3 n^3} \qquad (3.2.9)$$

where n is the refractive index of the medium.

From the above discussion it is clear that stimulated emission process competes with spontaneous emission and absorption process. In order to amplify a beam of light the rate of stimulated emission must be increased. This can be done by increasing N_2 and/or ρ_ν.

3.3 Absorption of radiation

Let us consider a collimated beam of perfectly monochromatic radiation of unit cross sectional area passing through an absorbing medium. We assume that there is only one relevant electron transition which occurs between the energy levels E_1 and E_2. The change in irradiance of the beam as a function of distance is given by

$$\Delta I(x) = I(x + \Delta x) - I(x)$$

For a homogeneous medium $\Delta I(x)$ is proportional to both the distance traveled and to I(x). That is $\Delta I(x) = -\alpha I(x)\Delta x$. The proportionality constant α is called *absorption coefficient*. The negative sign indicates the reduction in beam irradiance due to absorption, as α is a positive quantity. Writing this expression as a differential equation we get

$$\frac{dI(x)}{dx} = -\alpha I(x)$$

Integrating this equation we have

$$I = I_0 \exp(-\alpha x) \qquad (3.3.1)$$

where I_0 is the incident irradiance.

So, due to absorption the irradiance decreases exponentially with distance. If we can make α negative then $(-\alpha x)$ in the exponent of equation (3.3.1) becomes positive. So the beam irradiance grows as it propagates through the medium in accordance with the equation

$$I = I_0 \exp(kx) \tag{3.3.2}$$

Where $k = -\alpha$ is called the *small signal gain coefficient*. It can be shown that the expression of α is given by [31]

$$\alpha = \left(\frac{g_2}{g_1}N_1 - N_2\right)\frac{B_{21}h\nu n}{c} \tag{3.3.3}$$

where n is the refractive index of the medium. So the expression of k is

$$k = \left(N_2 - \frac{g_2}{g_1}N_1\right)\frac{B_{21}h\nu n}{c} \tag{3.3.4}$$

In order to make k positive N_2 must be greater than $\frac{g_2}{g_1}N_1$. As normally $\frac{g_2}{g_1} \cong 1$ then condition for beam amplification is $N_2 > N_1$. As E_2 is the upper energy level, normally population density in energy level E_2 is lower than that of E_1. So in order to get amplification, we need to create a non-equilibrium distribution of atoms among various energy levels of the atomic system. The non-equilibrium condition is called *population inversion*. In order to create population inversion a large amount of energy must be supplied to excite atoms to upper energy level. This excitation process is called *pumping*.

3.4 Optical feedback

Laser is more analogous to an oscillator than an amplifier. In an electronic oscillator, an amplifier tuned to a particular frequency is provided with positive feedback. When switched on, electrical noise signal of appropriate frequency appearing at the input will be amplified. The amplified output is fed back to the input and further amplified and so on. A stable output is quickly reached since the amplifier saturates at high input voltages.

In laser, positive feedback is obtained by placing the gain medium between a pair of mirrors which form an optical cavity (a Febry - Perot resonator). The initial stimulus is provided by any spontaneous transition between appropriate energy levels in which the emitted photon travels along the axis of the system. The signal is amplified as it passes through the medium and fed back by the mirrors. Saturation is reached when gain provided by the medium exactly matches the losses incurred during a complete round trip.

The gain per unit length of most active media is so small that very little amplification of a beam of light results from a single pass through the medium. But in the multiple passes, which a beam undergoes when the medium is placed within a cavity, the amplification may be substantial.

3.5 Threshold conditions

A steady state level of oscillation is reached when the rate of amplification is balanced by the rate of loss. This is the situation in continuous output lasers. In pulse laser the situation is little different. While population inversion is a necessary condition for laser action, it is not sufficient because the gain coefficient must be large enough to overcome the losses and sustain oscillations. The total loss of the system is due to a number of different processes such as

(i) Transmission at the mirrors - the transmission from one of the mirrors usually provides the useful output, the other mirror is made as reflective as possible to minimize losses.
(ii) Absorption and scattering at the mirrors
(iii) Absorption in the laser medium due to undesired transitions
(iv) Scattering at optical inhomogeneities in the laser medium
(v) Diffraction losses at the mirrors.

Let us include all the losses except those due to transmission at the mirrors in a single effective loss coefficient γ, which reduces the effective gain coefficient to $k-\gamma$. We can determine the threshold gain by considering the change in irradiance of

a beam of light undergoing a round trip within the laser cavity. Let us assume that the laser medium is placed between the mirrors M_1 and M_2, which have reflectances R_1 and R_2 and a separation L. Then in traveling from M_1 to M_2 the beam irradiance increases from I_0 to I where

$$I=I_0 \exp(k-\gamma)L .$$

After reflection at M_2 , the beam irradiance will be $R_2I_0 \exp(k-\gamma)L$ and after a complete round trip the final irradiance will be $R_1R_2I_0 \exp\{2(k-\gamma)L\}$. The ratio of final irradiance to initial irradiance is given by

$$G = \frac{\text{Final irradiance}}{\text{Initial irradiance}} = R_1R_2\exp\{2(k-\gamma)L\}$$

If G is greater than unity a disturbance at the laser resonant frequency will undergo a net amplification and the oscillations will grow. If G is less than unity the oscillations will die out. Therefore we can write the threshold condition as

$$G = R_1R_2\exp\{2(k_{th}-\gamma)L\} = 1 \qquad (3.5.1)$$

where k_{th} is the threshold gain. It is important to realize that the threshold gain is equal to the steady state gain in continuous output lasers, i.e. $k_{th} = k_{ss}$. This equity is due to a phenomenon known as *gain saturation*. In terms of population inversion there will be a threshold value $N_{th} = [N_2 - (g_2/g_1)N_1]_{th}$ corresponding to k_{th}. In steady state condition $[N_2 - (g_2/g_1)N_1]$ remains equal to N_{th} regardless of the amount by which the threshold pumping rate is exceeded. The small signal gain coefficient at threshold can be obtained from equation (3.5.1)

$$k_{th} = \gamma + \frac{1}{2L}\ln\left(\frac{1}{R_1R_2}\right) \qquad (3.5.2)$$

where the first term represents the volume losses and the second the loss in the form of useful output. The value of k_{th} can also be found from equation (3.3.4) as

$$k_{th} = \left(N_2 - \frac{g_2}{g_1}N_1\right)_{th} \frac{B_{21}h\nu n}{c}$$

$$= N_{th}\frac{B_{21}h\nu n}{c} \qquad (3.5.3).$$

Equations (3.5.2) and (3.5.3) show that k can have a wide range of values depending not only on $[N_2 - (g_2/g_1)N_1]$ but also on intrinsic properties of the active medium.

3.6 Lineshape function

So far we have assumed that all the atoms would be able to interact with the perfectly monochromatic beam. In fact this is not so. Spectral lines have a finite wavelength spread. This can be seen in both emission and absorption and if we are to measure transmission as a function of frequency for the transition between the two energy levels E_1 and E_2 we would obtain the bell-shape curve shown in Figure 3.2(a). The emission curve would be the inverse of this (see Figure 3.2(b)).

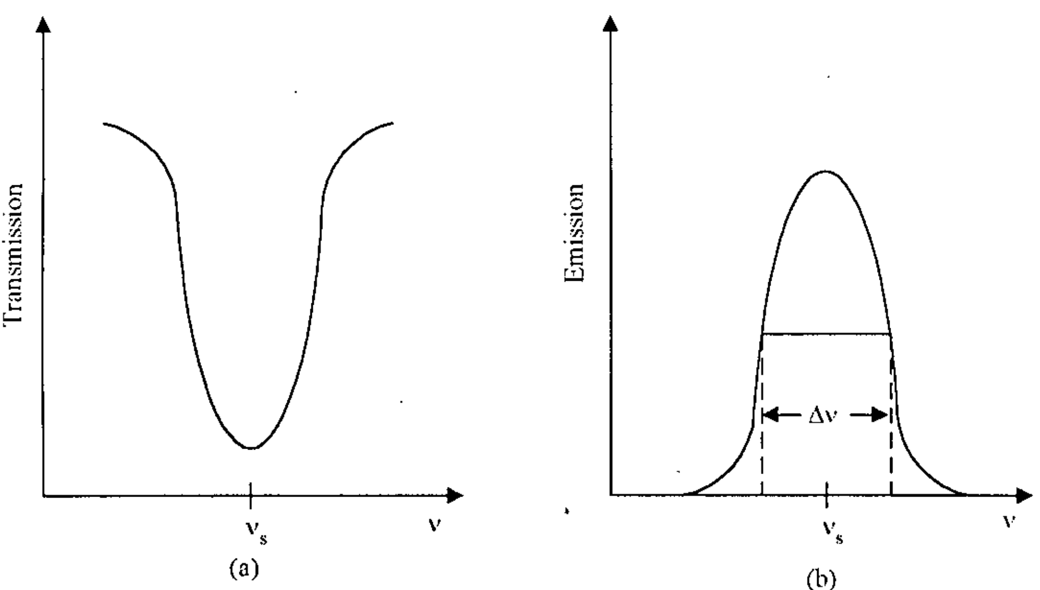

FIG. 3.2 (a) Transmission curve for transitions between two energy levels and (b) emission curve for transition between the energy levels.

The shape of these curves is described by *lineshape function* $g(\nu)$. $g(\nu)$ can also be used to describe a frequency probability curve. $g(\nu)d\nu$ may be defined as the probability that a given transition between the two energy levels will result in an emission or absorption of a photon whose frequency lies between ν and $\nu + d\nu$. $g(\nu)$ is normalized such that $\int_{-\infty}^{\infty} g(\nu) d\nu = 1$. Therefore a photon of energy $h\nu$ may not

necessarily stimulate another photon of energy $h\nu$. $g(\nu)d\nu$ can be taken as the probability that the stimulated photon will have an energy between $h\nu$ and $h(\nu + d\nu)$. When a monochromatic beam of frequency ν_s interacts with a group of atoms with a lineshape function $g(\nu)$, the small signal gain coefficient may be written as [31]

$$k(\nu_s) = \left(N_2 - \frac{g_2}{g_1} N_1 \right)_{th} \frac{B_{21} h\nu_s n g(\nu_s)}{c} \tag{3.6.1}$$

It can be shown that $g(\nu_s) = \frac{1}{\Delta\nu}$, where ν_s is the frequency at which the value of the function is maximum and $\Delta\nu$ is the linewidth, i.e., the separation between two points on the curve where the function falls to half of its peak value which occurs at ν_s.

The form of the lineshape function $g(\nu)$ depends on the particular mechanism responsible for *spectral broadening* in a given transition. The three most important mechanisms are Doppler broadening, collision (or pressure) broadening and natural (or lifetime) broadening.

3.7 Stimulated emission from Erbium in Silicon

As mentioned before, emission at 1.54 μm wavelength can be obtained from Er doped Si due to internal 4f shell transition of excited Er atoms from $^4I_{13/2}$ to $^4I_{15/2}$. The initial stimulus may be provided by electrically supplying a large number of electrons in the conduction band of Si. These electrons will recombine with holes in valence band via Er related levels and the recombination energy will excite Er atoms to first excited state ($^4I_{13/2}$). From this state a fraction of excited atoms will return to ground state ($^4I_{15/2}$) radiatively giving rise to emission of photons. The photons will stimulate the generation of more photons and soon laser oscillations will build up inside the cavity. Useful output may be obtained through one of the mirrors used in the cavity.

Chapter 4

Mathematical Model for Erbium Luminescence

In this chapter the mathematical model for excitation and de-excitation of Er atoms in Si will be presented. Equations for pumping and decay will be described for both steady state and time varying case. The model will also include stimulated emission and absorption in steady state. Finally, a practical laser diode using Er doped Si will be proposed and the expression of its output power will be obtained.

4.1 Steady state excitation and de-excitation mechanism

From the discussion in the previous chapters it is now clear that recombination of electron-hole pairs at Er related levels excites Er atoms in Silicon. It is now an accepted fact that Er introduces a level in the Silicon bandgap somewhat 0.15 eV below the conduction band [14,15,16,17]. This trap level captures electrons from the conduction band. If the electron occupied level can capture a hole before the electron is thermally dissociated, the corresponding Er^{3+} ion takes the recombination energy of the electron-hole pair and thus reaches its first excited state $^4I_{13/2}$.

Let,

N_{er} = total number of active Er sites per unit volume

n_{er} = total number of active Er sites filled by electrons at a steady state of optical excitation per unit volume

e_n = electron emission rate, s^{-1}

e_p = hole emission rate, s^{-1}

c_n = electron capture coefficient, cm^3-s^{-1}

c_p = hole capture coefficient, cm^3-s^{-1}

n = free electron concentration

p = free hole concentration

From the discussion in section 2.5 we can write

electron emission rate from Er related level = $(e_n + c_p p)n_{er}$ (4.1.1)

and electron capture rate by Er related level = $(e_p + c_n n)(N_{er} - n_{er})$ (4.1.2)

At steady state, electron emission rate = electron capture rate

$$(e_n + c_p p)n_{er} = (e_p + c_n n)(N_{er} - n_{er}) \tag{4.1.3}$$

Thus the fraction of Erbium sites occupied by electron is given by

$$f_t = \frac{n_{er}}{N_{er}} = \frac{e_p + c_n n}{e_n + e_p + c_n n + c_p p} \tag{4.1.4}$$

Now let,

n_{er}^* = total number of excited Er atoms at steady state per unit volume

$N_{er} - n_{er}^*$ = number of available Er sites for excitation at steady state per unit volume

When a trapped electron recombines with a hole before the electron gets dissipated thermally back to the conduction band, the recombination energy excites the corresponding Er atom. But, if an Er atom is already in the excited state due to previous recombination of electron-hole pair, the recombination energy will be wasted away. At steady state, $f_t N_{er}$ gives the density of electron occupied Er sites. So, the density of electron occupied Er sites available for excitation can be expressed by $f_t(N_{er} - n_{er}^*)$.

Thus the excitation rate, i.e., pumping rate per unit volume per second is given by

$$P = f_t c_p p(N_{er} - n_{er}^*) \tag{4.1.5}$$

Once excited, the Er atom can de-excite radiatively or non-radiatively. If the radiative decay lifetime is τ_{rad} then the radiative decay rate is given by $\frac{n_{er}^*}{\tau_{rad}}$ per unit volume per second.

The competing parallel non-radiative decay process, on the other hand, consists of i) Auger de-excitation with free carriers, ii) Auger de-excitation with carriers bound to donor (or acceptor) level and iii) the energy back transfer.

Non-radiative decay lifetime corresponding to Auger de-excitation with free carriers is given by [16]

$$\frac{1}{\tau_{Af}} = C_{Ae}n \quad \text{for n-type Si} \tag{4.1.6}$$

$$\text{and } \frac{1}{\tau_{Af}} = C_{Ah}p \quad \text{for p-type Si} \tag{4.1.7}$$

where τ_{Af} is the decay lifetime , C_{Ae} and C_{Ah} are Auger coefficients (in cm^3-s^{-1}) for free electrons and holes respectively.

For n-type material, electron density is given as the summation of optically generated carriers and the thermal equilibrium concentration. Hole concentration can be taken to be equal to the excess carrier density.

So, $n = n_{op} + n_{th}$

and $p = n_{op}$

where n_{op} and n_{th} are optically and thermally generated electron concentrations respectively. Here intrinsic carrier concentrations n_i and p_i are deliberately ignored as these are very small compared to other contributions to n and p.

Similarly for p-type material the free carrier concentrations in valence band and conduction band can be given by

$$p = n_{op} + p_{th}$$

and $n = n_{op}$,

where p_{th} is the density of holes per unit volume in thermal equilibrium.

Now from the discussion of section 2.4, decay lifetime corresponding to Auger de-excitation with bound carriers is given by

$$\frac{1}{\tau_{Ab}} = C_{Abe}(N_d - n_{th}) \text{ for n-type Si} \tag{4.1.8}$$

$$\text{and } \frac{1}{\tau_{Ab}} = C_{Abh}(N_a - p_{th}) \text{ for p-type Si} \tag{4.1.9}$$

where τ_{Ab} is the decay lifetime ,C_{Abe} and C_{Abh} are Auger coefficients for bound carriers (in cm^3-s^{-1}), and N_d and N_a are donor and acceptor concentrations respectively.

As discussed in section 2.4, non-radiative decay lifetime of Er atoms due to energy back transfer process is given by

$$\frac{1}{\tau_{bt}} = W_0 \exp\left(-\frac{0.15\,eV}{kT}\right) \tag{4.1.10}$$

where τ_{bt} is the corresponding lifetime, W_0 is a fitting parameter (in s^{-1}) , k is Boltzmann's constant (in eV/K) and T is absolute temperature (in K).

So the non-radiative decay time of Er atoms can be expressed as

$$\frac{1}{\tau_{nonrad}} = \frac{1}{\tau_{Af}} + \frac{1}{\tau_{Ab}} + \frac{1}{\tau_{bt}} \tag{4.1.11}$$

Thus the total lifetime of Er decay is given by

$$\frac{1}{\tau_{eq}} = \frac{1}{\tau_{rad}} + \frac{1}{\tau_{nonrad}} \tag{4.1.12}$$

Thus the de-excitation rate or decay rate per unit volume per second is given by

$$D = \frac{n^*_{er}}{\tau_{eq}} \tag{4.1.13}$$

Assuming no change in electronic property of the corresponding defect levels of excited Er atoms, the rate of excitation and de-excitation must be equal at steady state.

$$f_t c_p p(N_{er} - n_{er}^*) = \frac{n_{er}^*}{\tau_{eq}} \qquad (4.1.14)$$

So at steady state the number of excited Er atoms per unit volume is given by

$$n_{er}^* = \frac{f_t c_p p}{f_t c_p p + \frac{1}{\tau_{eq}}} N_{er}$$

$$= \frac{(e_p + c_n n) c_p p}{(e_p + c_n n) c_p p + (e_n + e_p + c_n n + c_p p)\frac{1}{\tau_{eq}}} N_{er} \qquad (4.1.15)$$

The luminescence from Er is thus given by

$$I \, \alpha \, \frac{n_{er}^*}{\tau_{rad}} \qquad (4.1.16)$$

4.2 Time dependent rise of Erbium luminescence

When a laser pulse is applied to an Er doped Si sample, excess electron-hole pairs are generated almost instantly. However, rate of capture and emission of carriers through Er sites are controlled by corresponding emission and capture coefficients. As a result, a finite amount of time is needed for the Er luminescence to reach the steady state. In this case, both the number of electron occupied Er sites and that of excited Er atoms are functions of time. In order to find out the time dependent luminescence, i.e., number of excited Er atoms, the time equation for electron occupied Er sites is to be solved first. Then the corresponding time dependent Er luminescence can be determined by solving the rate equation of excited Er atoms.

4.2.1 Time dependent electron occupied Erbium states

We know form equations (4.1.1) and (4.1.2) that

$$\text{electron emission rate} = (e_n + c_p p) n_{er}(t) \qquad (4.2.1.1)$$

$$\text{electron capture rate} = (e_p + c_n n)(N_{er} - n_{er}(t)) \qquad (4.2.1.2)$$

So, the rate of change of electron occupied trap density at time t is given by

$$\frac{dn_{er}(t)}{dt} = (e_p + c_n n)(N_{er} - n_{er}(t)) - (e_n + c_p p)n_{er}(t)$$

$$\Rightarrow \frac{dn_{er}(t)}{dt} + an_{er}(t) = bN_{er} \qquad (4.2.1.3)$$

where,

$$a = e_p + e_n + c_n n + c_p p\,,$$

$$b = e_p + c_n n$$

Integrating factor $= e^{\int a\,dt} = e^{at}$

So the solution of the above differential equation is

$$n_{er}(t) = \frac{b}{a}N_{er} + Ce^{-at} \qquad (4.2.1.4)$$

where, C is an integration constant. Putting initial condition $n_{er}(0) = 0$, we get

$$C = -\frac{b}{a}N_{er} \qquad (4.2.1.5)$$

So, the time varying equation of electron occupied Er states is

$$n_{er}(t) = \frac{b}{a}N_{er}(1 - e^{-at}) \qquad (4.2.1.6)$$

4.2.2 Time dependent Erbium luminescence

The excitation and de-excitation rates are in this case time dependent. The excitation rate is $f_t(t)(N_{er} - n^*_{er}(t))c_p p$ as before with one exception that f_t and n^*_{er} are time dependent. Similarly de-excitation rate is $\frac{n^*_{er}(t)}{\tau_{eq}}$. So increase in number of excited Er atoms per second, i.e., the rate of change of excited Er is given by

$$\frac{dn^*_{er}(t)}{dt} = f_t(t)(N_{er} - n^*_{er}(t))c_p p - \frac{n^*_{er}(t)}{\tau_{eq}}$$

$$= \frac{n_{er}(t)}{N_{er}}(N_{er} - n^*_{er}(t))c_p p - \frac{n^*_{er}(t)}{\tau_{eq}} \qquad (4.2.2.1)$$

where, $n_{er}(t)$ is given by equation (4.2.1.6)

The exact analytical solution of this differential equation will be complicated. So numerical solution of the differential equation using fifth order RK method with an initial condition of $n^*_{er}(0) = 0$ will be obtained in this case.

4.3 Decay profile of Erbium luminescence

When the laser pulse is switched off the number of excited Er atoms starts to decrease. As a consequence, the strength of Er luminescence gradually decays to zero. Here again, to find out the time dependent luminescence, the time equation for electron occupied Er sites is to be solved first. Then the corresponding time dependent Er luminescence can be determined by solving the rate equation of excited Er atoms. As in section 4.2, both the number of electron occupied Er sites and that of excited Er atoms are time varying. In addition, concentrations of free electrons and holes also are functions of time.

The rate of change of electron occupied Er sites is given by

$$\frac{dn_{er}(t)}{dt} = (e_p + c_n n(t))(N_{er} - n_{er}(t)) - (e_n + c_p p(t))n_{er}(t) \qquad (4.3.1)$$

Here n(t) and p(t) are time dependent free electron and hole concentrations respectively. Whenever the laser pulse is switched off, optically generated carrier concentration starts to decrease exponentially. If the optically generated carrier concentration is n_{op} just before the termination of laser pulse, i.e., at steady state condition then n(t) and p(t) are given by

$$n(t) = n_{th} + n_{op}e^{-t/\tau} \text{ and } p(t) = n_{op}e^{-t/\tau} \text{ for n-type material}$$

and $n(t) = n_{op}e^{-t/\tau}$ and $p(t) = p_{th} + n_{op}e^{-t/\tau}$ for p-type material,

where τ = lifetime of free carriers.

The rate of change of excited Er atoms is given by

$$\frac{dn^*_{er}(t)}{dt} = f_t(t)(N_{er} - n^*_{er}(t))c_p p(t) - \frac{n^*_{er}(t)}{\tau_{eq}}$$

$$\Rightarrow \frac{dn^*_{er}(t)}{dt} = \frac{n_{er}(t)}{N_{er}}(N_{er} - n^*_{er}(t))c_p p(t) - \frac{n^*_{er}(t)}{\tau_{eq}} \qquad (4.3.2)$$

In order to solve equation 4.3.2, analytical solution of equation 4.3.1 is needed. But the solution of equation (4.3.1) is itself a complex one due to time varying carrier concentration. So techniques for numerically solving simultaneous differential equations will be employed in this case (see flowchart in Appendix A). The steady state condition prior to termination of laser pulse will be used for calculation of initial values of n_{er} and n^*_{er}.

4.4 Stimulated emission from Erbium in Silicon

While calculating the Er luminescence in sections 4.1–4.3, only spontaneous emission has been considered. If we want to incorporate stimulated emission and absorption, corresponding excitation and de-excitation rates are to be included in the rate equations.

The stimulated excitation rate is proportional to density of unexcited Er atoms and power density.

So stimulated excitation rate = $(N_{er} - n^*_{er})\rho_v B_{12}$,

where B_{12} is a constant and ρ_v is power density which is given by $\rho_v = Nh\nu$. Here N is number of photons per unit volume having frequency ν.

Similarly stimulated emission rate is proportional to number of excited Er atoms and power density.

Thus stimulated de-excitation rate = $n^{*}_{er}\rho_v B_{21}$.

So the modified rate equations are :

excitation rate = $f_t c_p p(N_{er} - n^{*}_{er}) + (N_{er} - n^{*}_{er})\rho_v B_{12}$ (4.4.1)

de-excitation rate = $\dfrac{n^{*}_{er}}{\tau_{eq}} + n^{*}_{er}\rho_v B_{21}$ (4.4.2)

At steady state these two rates must be equal. So

$$f_t c_p p(N_{er} - n^{*}_{er}) + (N_{er} - n^{*}_{er})\rho_v B_{12} = \frac{n^{*}_{er}}{\tau_{eq}} + n^{*}_{er}\rho_v B_{21} \quad (4.4.3)$$

Now the photon generation rate and decay rate can be equated at steady state. Hence

$$(N_{er} - n^{*}_{er})\rho_v B_{12} = \frac{n^{*}_{er}}{\tau_{rad}} + n^{*}_{er}\rho_v B_{21} \quad (4.4.4)$$

If $B_{12} = B_{21}$ then we get

$$\rho_v B_{21} = \frac{n^{*}_{er}}{\tau_{rad}(N_{er} - 2n^{*}_{er})} \quad (4.4.5)$$

Putting this value in equation (4.4.3) we have (detailed derivation is given in Appendix B)

$$n^{*}_{er} = \frac{f_t c_p p}{f_t c_p p + \dfrac{1}{\tau_{eq}} - \dfrac{1}{\tau_{rad}}} N_{er} \quad (4.4.6)$$

4.5 Condition for LASER action – threshold

Below and at threshold the value of ρ_v can be neglected since lasing has not yet occurred. So equation (4.1.14) can be used instead of equation (4.4.3) to obtain the expression of excess carrier density at threshold and at low temperature condition where n = p. Thus

$$f_t c_p n_{thrs}(N_{er} - n^{*}_{er}) = n^{*}_{er}\left(\frac{1}{\tau_{rad}} + \frac{1}{\tau_{Ab}} + \frac{1}{\tau_{bt}} + C_{Af} n_{thrs}\right)$$

$$\Rightarrow n_{thrs}\left\{f_t c_p (N_{er} - n_{er}^*) - n_{er}^* C_{Af}\right\} = n_{er}^*\left(\frac{1}{\tau_{rad}} + \frac{1}{\tau_{Ab}} + \frac{1}{\tau_{bt}}\right)$$

$$\Rightarrow n_{thrs} = \frac{n_{er}^*\left(\frac{1}{\tau_{rad}} + \frac{1}{\tau_{Ab}} + \frac{1}{\tau_{bt}}\right)}{f_t c_p (N_{er} - n_{er}^*) - n_{er}^* C_{Af}} \quad (4.5.1)$$

where, n_{thrs} = excess carrier density at threshold and $C_{Af} = C_{Ae}$ for n type material and $C_{Af} = C_{Ah}$ for p type material. Though according to equation (4.1.4) f_t is a function of n and p, at low temperature it will be a constant as values of e_n and e_p are negligible compared to $c_n n$ and $c_p p$. So, from equation (4.1.4) f_t can be approximated at low temperature as

$$f_t = \frac{n_{er}}{N_{er}} \cong \frac{c_n}{c_n + c_p} \quad (4.5.2)$$

which is definitely a constant quantity at a particular temperature.

Now, from equation (4.4.3) the expression of ρ_v can be written as

$$\rho_v = \frac{f_t c_p p (N_{er} - n_{er}^*) - \frac{n_{er}^*}{\tau_{eq}}}{B_{21}(2n_{er}^* - N_{er})} \quad (4.5.3)$$

From threshold the value of n_{er}^* becomes fixed as the system must reach at steady state condition. If input power is increased, number of free carriers (n and p) will increase which will decrease τ_{eq}. So above threshold the only parameters in the expression of ρ_v dependent on input power are p and τ_{eq}. Here $p = n_{thrs} + \Delta n$ where Δn is the value of excess carrier density in excess of the threshold value.

4.6 A proposed laser device using Erbium doped Silicon

4.6.1 Structure

A practical laser device may be constructed using a p - n^+ junction diode of Er doped Si. When the diode is forward biased a large number of minority carriers are injected into both sides of the junction. These minority carriers can take part in the

excitation mechanism of Er atoms. We have chosen p - n^+ junction so that the minority carriers involved are mainly electrons injected into p side. From the metallurgical junction a layer of p region is doped with Er. The length of Er doped region, L_{er} is chosen in such a way that it remains well within the diffusion length, L_D. This will ensure that there are always enough free carriers to participate in the excitation process.

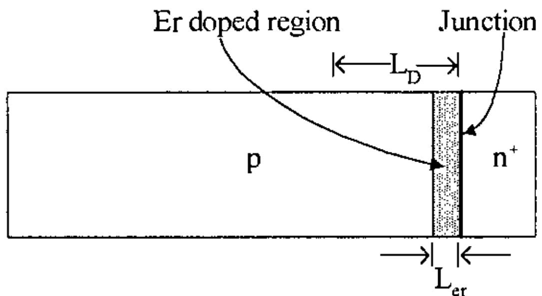

FIG. 4.1 Proposed p-n^+ junction diode laser

When the diode is forward biased, Er atoms are excited through carrier-mediated process and a fraction of these decay radiatively producing photons of fixed frequency. These photons can interact with excited and unexcited Er atoms giving rise to stimulated emission and absorption. If the injected carrier concentration becomes large enough, the stimulated emission can exceed the absorption so that optical gain can be achieved in Er doped region. When the round trip gain will exceed the total loss over the same distance, laser oscillation will occur.

The additional carriers present in the Er doped region will increase its refractive index above that of the surrounding material. So a dielectric waveguide layer will be formed which will confine the radiation well within the Er doped region. Though there will be some spreading out of the radiation into the surrounding lossy Si, we will neglect this effect to simplify our calculation.

Using the structure discussed a laser cavity may be formed by placing mirrors at both the ends of the diode as shown in the fig. 4.2. Mirrors can be cleaved flat edge or bragg reflectors.

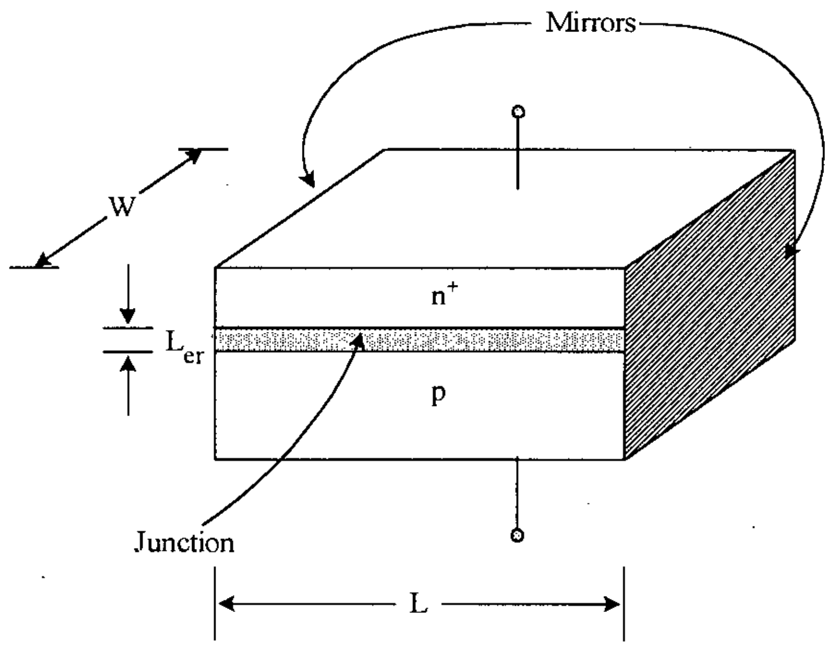

FIG. 4.2 An optical cavity using the proposed diode laser

4.6.2 Formulation

Let,

n = average concentration of electrons injected into the Er doped region

τ = lifetime of the injected carriers

A = cross sectional area of the junction, W $\times$ L.

Electron injection rate = $\frac{n}{\tau}$ per unit volume per sec.

So electron injection rate into the total volume of Er doped region = $\frac{n}{\tau} A L_{er}$ per sec.

Charge injected into the volume per sec, i.e., current $I = \frac{n}{\tau} A L_{er} q$. (4.6.2.1)

Current density $J = \frac{I}{A} = \frac{n}{\tau} L_{er} q$. (4.6.2.2)

At threshold the expression becomes

$$J_{thrs} = \frac{n_{thrs}}{\tau} L_{cr} q \,. \qquad (4.6.2.3)$$

where n_{thrs} = injected electron concentration at threshold.

As the injection current increases above threshold, laser oscillations build up and the population inversion is clamped at the threshold value.

Output power from the optical cavity is directly proportional to ρ_v. So equations (4.6.2.2) and (4.6.2.3) along with equations (4.5.1) and (4.5.3) will be used to evaluate the dependence of output power of the proposed laser device on current density above threshold.

Chapter 5

Results and Discussion

In chapter four the behavior of Er luminescence under different conditions has been analyzed. The analysis has been made for steady state and time varying conditions of spontaneous emission, for effect of short excitation pulse and for steady state stimulated emission and absorption. In this chapter results of these analysis, their significance and the effect of different parameters such as doping level, temperature, excitation level etc. on Er luminescence will be discussed. Also the feasibility of obtaining laser from the laser device proposed in section 4.6 will be studied.

5.1 Parameters for Erbium incorporated Silicon

Whenever Silicon is doped with an impurity, a trap level is formed in Silicon bandgap. It has been reported [14,15,16,17] that Erbium introduces a trap level at around 0.15 eV below the Silicon conduction band which is responsible for the excitation mechanism. So 0.15 eV has been used as activation energy [16]. The values of electron emission coefficient and hole emission coefficient have been calculated from the paper of S. Libertino et al. [14]. The electron and hole emission coefficients are given by

$$e_n = Ae^{-\frac{E_a}{kT}} \tag{5.1.1}$$

$$e_p = Ae^{-\left(\frac{E_g-E_a}{kT}\right)} \tag{5.1.2}$$

where,

E_g = Silicon bandgap energy, 1.1 eV

E_a = activation energy, 0.15 eV

k = Boltzmann's constant eV/K

T = temperature K

A = constant, $7.43\times10^{10}\ s^{-1}$.

The electron capture coefficient, $c_n = \sigma_n V_{th}$ (5.1.3)

The hole capture coefficient, $c_p = \sigma_p V_{th}$ (5.1.4)

where,

$$V_{th} = \text{thermal velocity} = \sqrt{\frac{3kT}{m^*}}$$

σ_n = electron capture cross section area

σ_p = hole capture cross section area

m^* = effective mass of electron or hole

The electron and hole capture cross sections have been taken as $2.2\times10^{-19}\ cm^2$ [3]. Electron and hole effective masses are taken as $m_e^* = 1.1m_0$ and $m_h^* = 0.56m_0$, where m_0 is the electron rest mass, 9.1095×10^{-31} Kg. [32].

In order to find out the value of thermally generated carrier density we used the expressions used in Priolo et al. [16]. The contribution of shallow donor or acceptor level to free electron or hole density respectively can be approximated by

$$n_{th} \cong \left(\frac{N_d N_c}{2}\right)^{1/2} \exp\left(-\frac{\varepsilon_d}{2kT}\right) \qquad (5.1.5)$$

and $$p_{th} \cong \left(\frac{N_a N_v}{2}\right)^{1/2} \exp\left(-\frac{\varepsilon_a}{2kT}\right) \qquad (5.1.6)$$

where N_d (N_a) is the donor (acceptor) concentration, N_c (N_v) is density of states in the conduction (valence) band and ε_d (ε_a) is the dissociation energy of the shallow donor (acceptor) level. The expressions of N_c and N_v have been taken from [32] which are as follow

$$N_c = 2\left(\frac{2\pi m_n^* kT}{h^2}\right)^{3/2} \qquad (5.1.7)$$

$$N_v = 2\left(\frac{2\pi m_p^* kT}{h^2}\right)^{3/2} \tag{5.1.8}$$

where

m_n^* = electron effective mass

m_p^* = hole effective mass

h = Plank's constant

We have assumed Phosphorous doping in n-type Silicon and Boron doping in p-type Silicon. Both the donor level of P and acceptor level of B have an energy of 45 meV [16]. So the values of ε_d and ε_a are equal to 0.045 eV.

For optical excitation, 514.5 nm laser having a spot diameter of 3 mm and penetration depth of 1 μm have been used. In order to find out the contribution of optical excitation to excess carrier concentrations in conduction band and valence band, we need to calculate the optical generation rate first. If we assume 100% absorption efficiency then optical generation rate is given by

$$g_{op} = \frac{P/V}{h\nu} \quad cm^{-3}\, s^{-1} \tag{5.1.9}$$

and the optically generated carrier concentration

$$n_{op} = p_{op} = g_{op} \times \tau = \frac{P/V}{h\nu} \times \tau \ \text{ per } cm^3 \tag{5.1.10}$$

where

P = power supplied by laser, Watt

V = $\pi r^2 d$ = volume penetrated by laser, cm^3

h = Plank's constant, J-s

ν = frequency of photon

τ = lifetime of excess carrier.

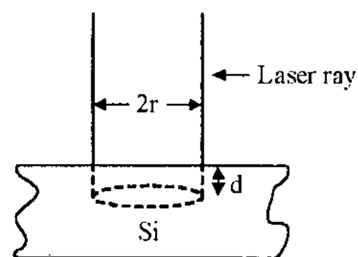

Throughout our calculation we have neglected the value of intrinsic carrier density as it is very small ($\approx 10^{10}$ /cm^3 at 300° K) compared to typical optically generated carrier concentration ($\approx 10^{17}$ /cm^3).

Lower value of τ is expected at higher temperature. This is due to the fact that, only a fraction of optically generated carriers recombine through Erbium related levels. It is however worth mentioning that the decay rate of excess carriers $\frac{n_{op}}{\tau}$ must be greater than the recombination rate $f_t c_p p N_{er}$ through Erbium related levels at any temperature.

Values of other parameters used are

$\tau_{rad} = 0.001$ s as stated in Xie et al. [13]

$C_{Ae} = 2.4\times10^{-13}$ cm^3 s^{-1} as proposed in Priolo et al. [16]

$C_{Abe} = 1.9\times10^{-14}$ cm^3 s^{-1} [16]

$C_{Ah} = 6.6\times10^{-14}$ cm^3 s^{-1}

$C_{Abh} = 6.5\times10^{-15}$ cm^3 s^{-1} [16]

$W_0 = 10^9$ s^{-1} [16,21].

The value of C_{Ah} has been slightly modified from the value proposed in [16] which is 2.4×10^{-13} cm^3 s^{-1}. This is done to fit the calculated data with the experimentally obtained data. The value, however is consistent with the fact that the Auger effect with free carriers is weaker in p-type Si than in n-type Si as suggested by [16].

Unless otherwise specified the following values have been used for calculation of PL intensity

$T = 9°$ K, $N_{er} = 10^{17}$ per cm^3 and $N_d = 4.0\times10^{17}$ per cm^3.

5.2 Erbium luminescence as a function of excitation

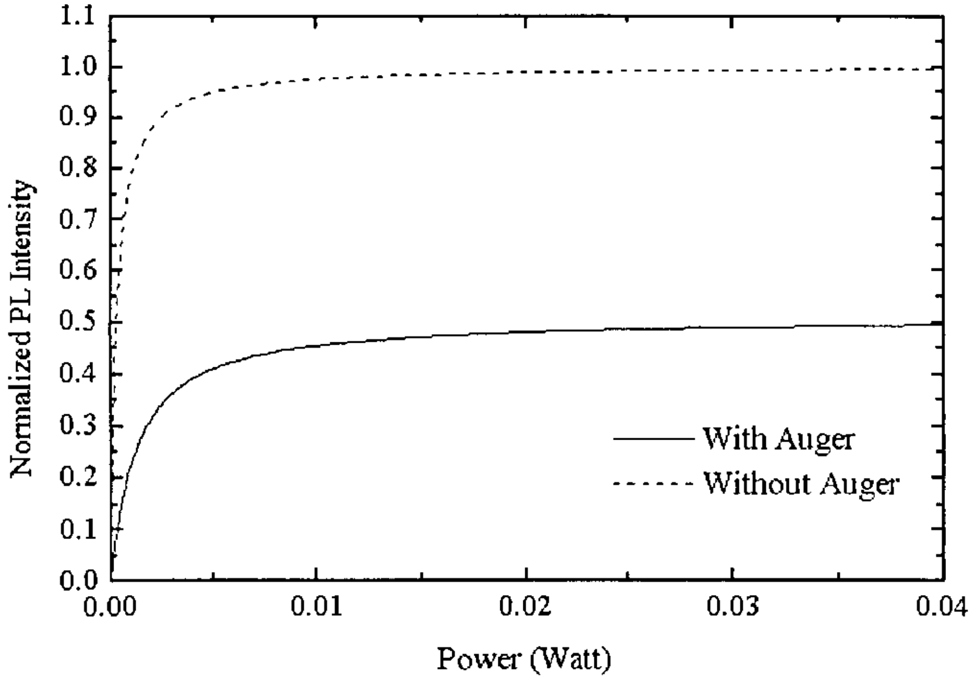

FIG. 5.1 Calculated PL intensity profile from Erbium under variable photo-excitation. Typical values of N_{er} , N_d and T have been used. Excess carrier lifetime has been taken as 40 μs.

From the discussion of the operation of reverse biased Si:Er LEDs in section 2.6, it can be said that impurity Auger process plays a dominant role in non-radiative de-excitation processes of Er in Si. Our model includes the effects of impurity Auger process with free and bound carriers and the energy back transfer mechanism. Figure 5.1 shows the result of inclusion of Auger effect with both free carriers and bound carriers. Energy back transfer process is negligible here as temperature is very low (9° K). The inclusion of Auger effect causes an increase in non-radiative Er decay rate which is responsible for the reduced PL intensity. Inclusion of Auger effect is important in Si:Er luminescence as doping levels are typically high. The saturation of PL intensity at higher excitation power has been shown experimentally by Palm et al. [19] and Coffa et al. [20]. It can be explained by the fact that at higher excitation level the radiative efficiency decreases due to increased non-radiative decay processes [19,20].

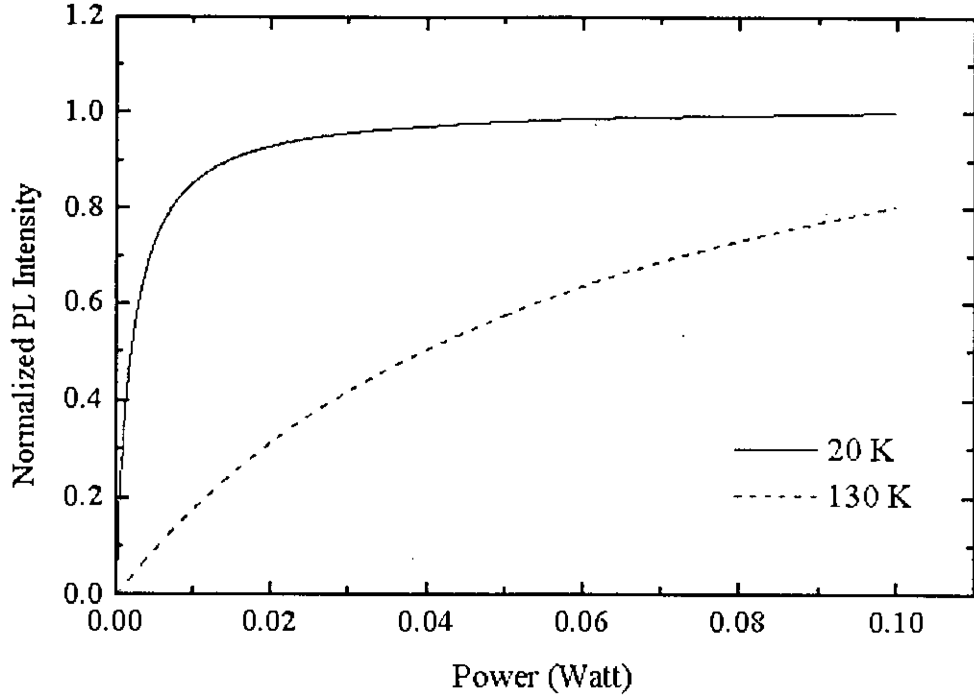

FIG. 5.2 Calculated PL intensity profile under variable photo-excitation at two different temperatures. Typical values of N_{er} and N_d have been used. Excess carrier lifetime has been taken as 20 μs at 20 K and 1 μs at 130 K.

Figure 5.2 shows the PL intensity vs. excitation power profile at two different temperatures. At higher temperature thermally generated carriers increase non-radiative Auger processes. But the stronger effect is the non-radiative energy back transfer which sets in at higher temperature [16,19]. According to Priolo et al. [16] the high temperature quenching can be best explained by impurity Auger process upto temperature 150° K as most of the shallow levels are ionized at this temperature. Above this temperature it can be best explained by energy back transfer process. As discussed in section 2.4, energy back transfer is a phonon-assisted process. So this non-radiative de-excitation process is expected to be thermally activated [16]. [16,19,21] have reported experimental evidence of similar phenomenon as shown in Fig. 5.2.

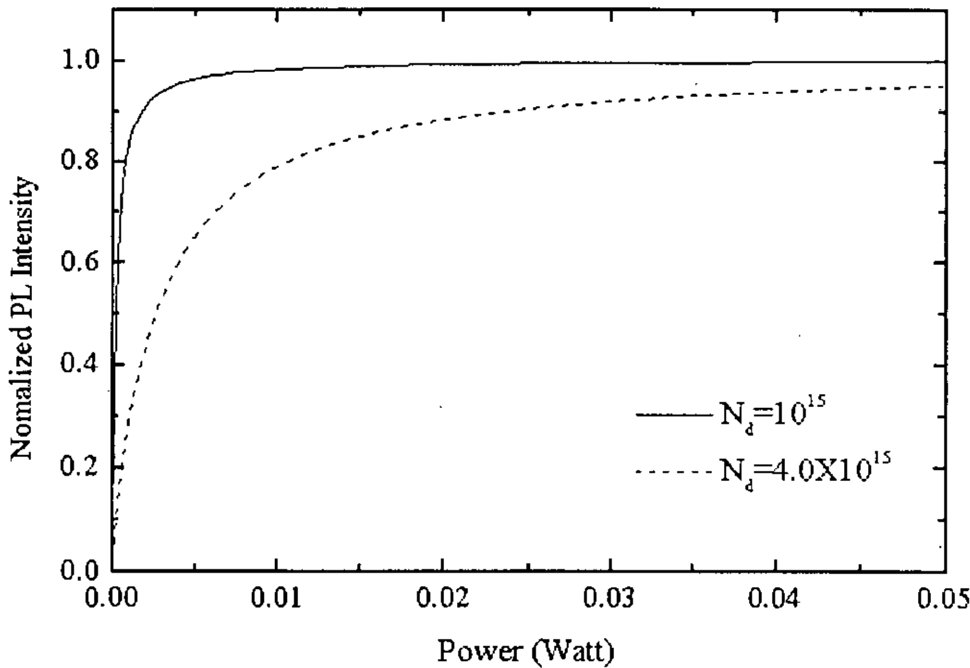

FIG. 5.3 Calculated PL intensity profile under variable photo excitation at two different donor doping levels. $N_{er} = 10^{17}$ per cm^3 and T =40 K have been used. Excess carrier lifetime has been taken as 18.5 μs for $N_d = 10^{15}$ per cm^3 and 11.5 μs for $N_d = 4\times10^{17}$ per cm^3.

Figure 5.3 shows PL intensity vs. excitation profile at two different background-doping levels. Here also the PL intensity decreases at higher doping level. Auger effect with carriers bound to donor (or acceptor) level increases with increasing doping level. Also at higher doping level the contribution of shallow donor (or acceptor) level to thermally generated excess carrier density increases. An increase in excess carrier density results in higher non-radiative decay rate via impurity Auger process with free carriers. Figure 5.3 is in agreement with experimental observation [16].

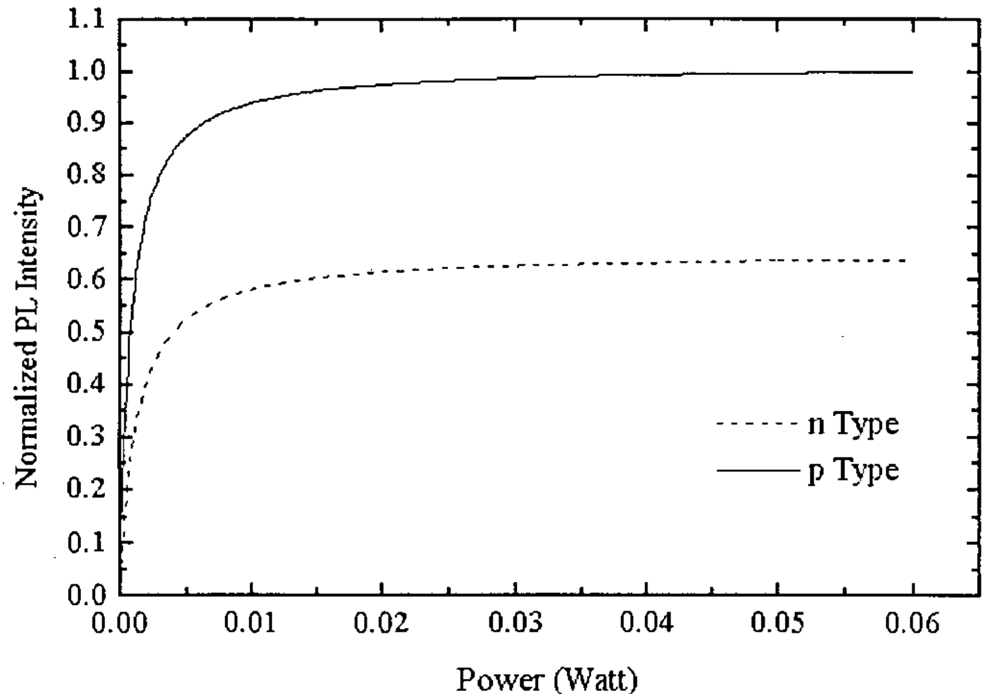

FIG. 5.4 Calculated PL intensity profile under variable photo excitation in n-type and p-type Silicon. Typical values of N_{er} and T have been used. $N_d = N_a = 10^{17}$ per cm^3 have been used. Excess carrier lifetime has been taken as 40 μs.

It is experimentally shown in [16] that for similar level of background doping, PL intensity obtained from p-type Si is greater than that from n-type Si. [16] suggested that Auger effect is less dominant in p-type material. We have incorporated this effect in our model by taking smaller value of Auger coefficient for p-type material than that for n-type material. Figure 5.4 shows that according to our model p-type material is capable of producing more PL intensity.

5.3 Erbium luminescence as a function of temperature

Excess carrier lifetime in Er doped Si depends on material processing, and also on the measuring temperature. In general, higher temperature introduces stronger non-radiative recombination routes with simultaneous reduction of the lifetime. No expression of lifetime in terms of temperature is however available for Er doped Si. It has been found in our model that the carrier lifetime is to be decreased with

increasing temperature in order to satisfy the relationship $\frac{n_{op}}{\tau} > f_t c_p p N_{er}$. We used lifetime variation with temperature in a fashion shown in Figure 5.5 to obtain

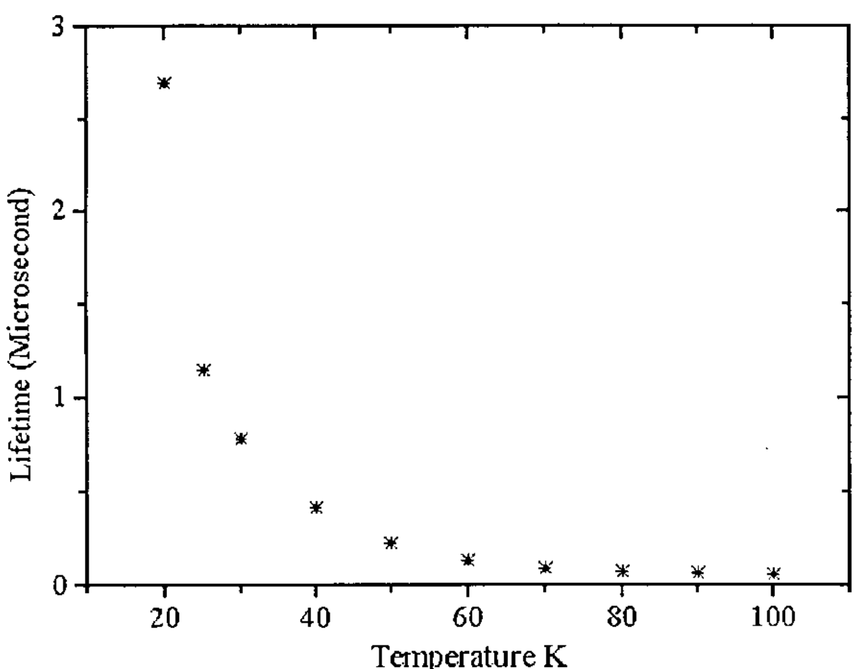

FIG. 5.5 Suggested dependence of excess carrier lifetime on temperature

PL intensity vs. reciprocal of temperature profile as shown in Figure 5.6. Such pattern of lifetime variation is expected due to small dissociation energy of free and bound excitons. The calculated profile is plotted against experimental data [33]. The same experimental conditions have been used in calculation with one exception. The sample used in the experiment had an Er concentration of 8×10^{18} per cm^3. But with such a high concentration, not all the Er sites are electrically or optically active [20]. We used a value of 10^{18} per cm^3 as the active Er concentration. It is evident that by using the suggested lifetime dependence on temperature excellent matching with the experimental data can be obtained. The relatively slow decrease of PL intensity upto 90° K can be attributed to impurity Auger processes while above that back transfer begins to dominate the non-radiative decay process.

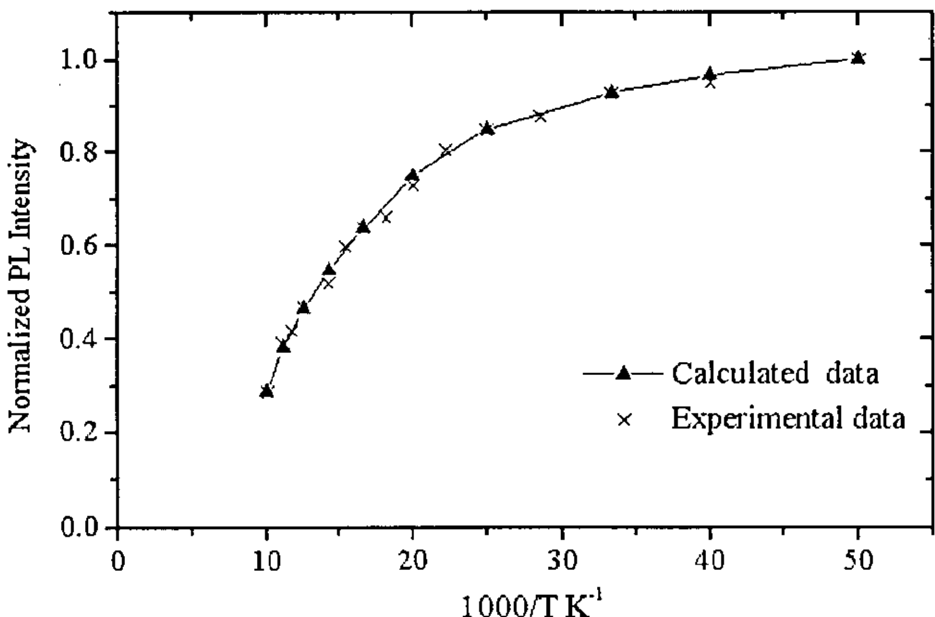

FIG. 5.6 Calculated PL dependence on temperature under constant photo-excitation using previously suggested dependence of lifetime on temperature. $N_{er}=10^{18}$ per cm^3 and $N_d=10^{16}$ per cm^3 have been used.

5.4 Photoluminescence decay profile

Our model can effectively explain the effects of some parameters such as temperature, background-doping level and type of material (n-type and p-type) on the decay profile of Er luminescence in Si. The effects obtained by our model have been experimentally found by Priolo et al. [16]. The following three figures demonstrate the observed effects.

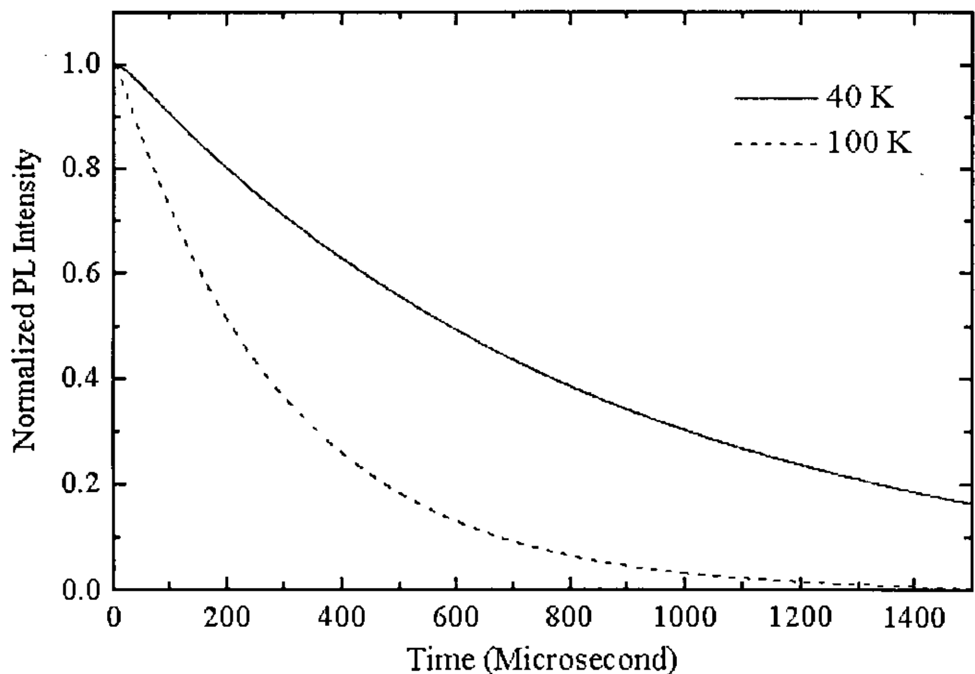

FIG. 5.7 Calculated PL decay profile at two different temperatures. $N_{er} = 10^{17}$ and $N_d = 10^{16}$ per cm^3 have been used. Excess carrier lifetime has been taken as 17 μs at 40 K and 5.5 μs at 100 K. Laser power of 1mW was used for steady state excitation. Curves have been normalized to initial values.

Figure 5.7 shows the decay profile of Er luminescence at two different temperatures. Sharper decay at higher temperature is observed. With increasing temperature impurity Auger effect with free carriers and energy back transfer increases which increase non-radiative decay rate of excited Er atoms. That explains the nature of the curves shown in Figure 5.7. It should be mentioned here that for all the decay profiles presented here the magnitude of PL intensities are different for different conditions. Within a plot the intensities have been normalized to initial values in order to better demonstrate the nature of decay of intensity.

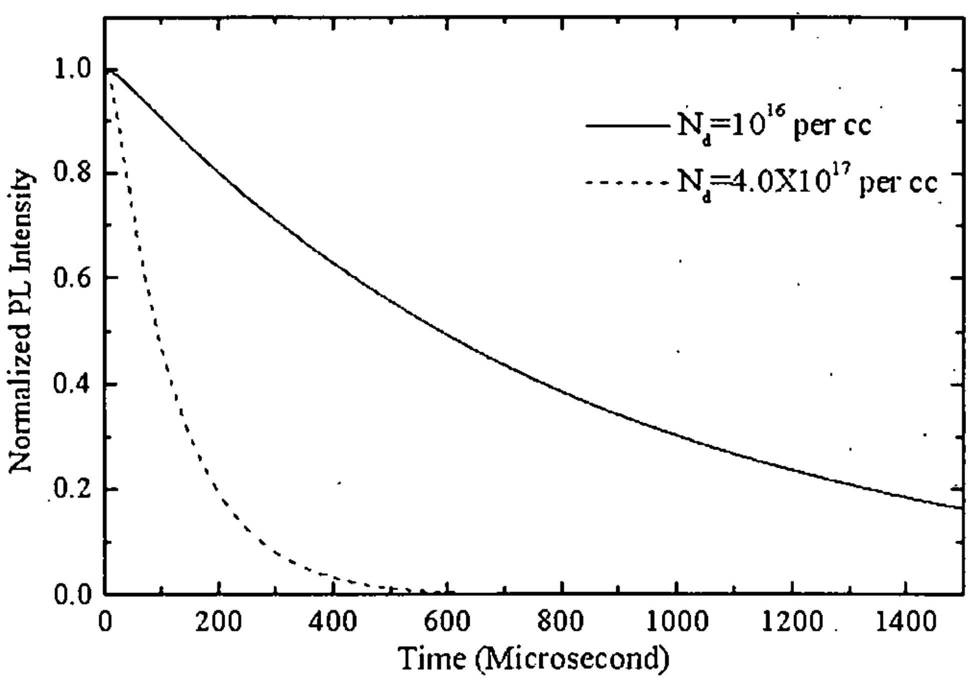

FIG. 5.8 Calculated luminescence decay profile at two different donor doping levels. $N_{cr}=10^{17}$ per cm^3 and T = 40 K have been used. Excess carrier lifetime has been taken as 17 μs at $N_d = 10^{16}$ per cm^3 and 12 μs at $N_d = 4\times10^{17}$ per cm^3. Laser power of 1mW was used for steady state excitation.

In Figure 5.8 the effect of background doping on decay profile has been demonstrated. With increasing doping level Auger process with bound carriers increases. Also thermally generated carrier density increases which in turn increases the impurity Auger process with free carriers. So non-radiative decay process becomes stronger which causes sharp reduction of the PL intensity.

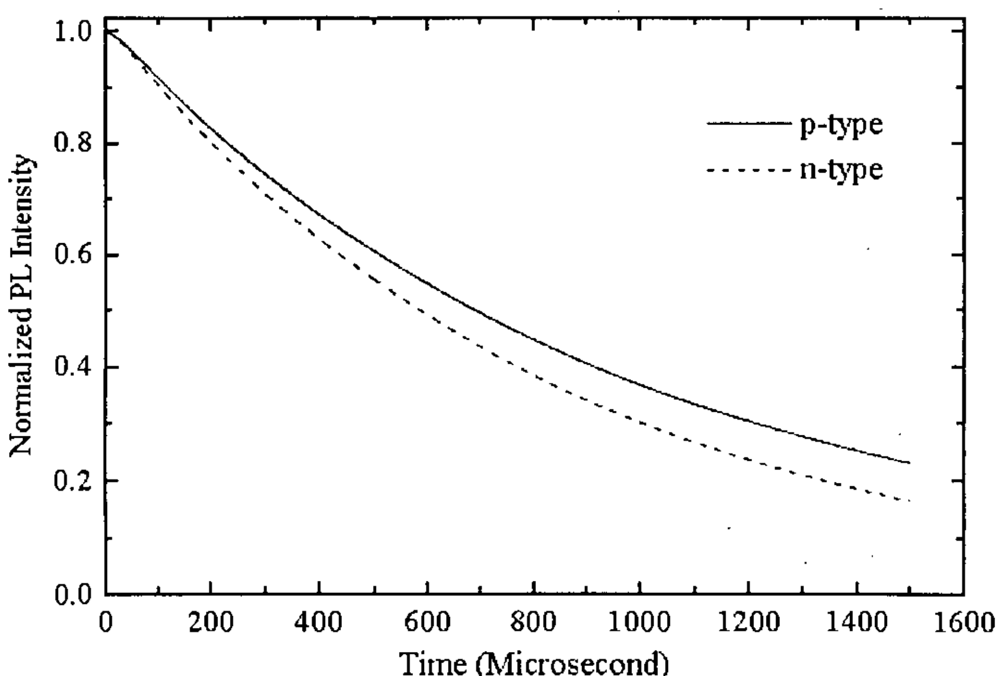

FIG. 5.9 Calculated PL decay profile for n-type and p-type Silicon. $N_{er} = 10^{17}$, $N_d = N_a = 10^{16}$ per cm^3, T = 40 K and τ = 17 μs have been used. Laser power of 1mW was used for steady state excitation.

Figure 5.9 shows the decay pattern in both n-type and p-type Si. As proposed by [16] the impurity Auger effects with both free carriers and bound carriers are weaker in p-type Si than in n-type Si. So higher decay rate in n-type Si is expected provided all other conditions remain same. Similar effect has been observed by [16].

5.5 Effect of short excitation pulse on Erbium luminescence

It has been reported in literature [17] that if an excitation pulse of short duration (30 μs) is applied on an Er doped specimen, the PL intensity continues to increase for some time even after the termination of the pulse. Huda et al. [3] gave the first physical explanation of the extended rise of luminescence and proposed a mathematical model of Er luminescence mechanism which is able to show the same phenomenon mathematically. The model presented in [3], although shows good

matching with experimental results at low temperature, has some limitations. Effects of impurity Auger process and the back transfer mechanism were not included in their model. Detailed behavior of Er luminescence under short excitation pulse and effects of temperature, excitation etc. have been explained by the present model.

Whenever a laser pulse is applied excess carriers are generated almost instantly. But the rate of Er excitation, i.e., pumping through sequential capture of electrons and holes by Er sites is controlled by corresponding emission and capture coefficients. So a finite amount of time is needed for the Er luminescence to reach steady state condition. This has been shown in Figure 5.10 along with corresponding pumping and decay rates.

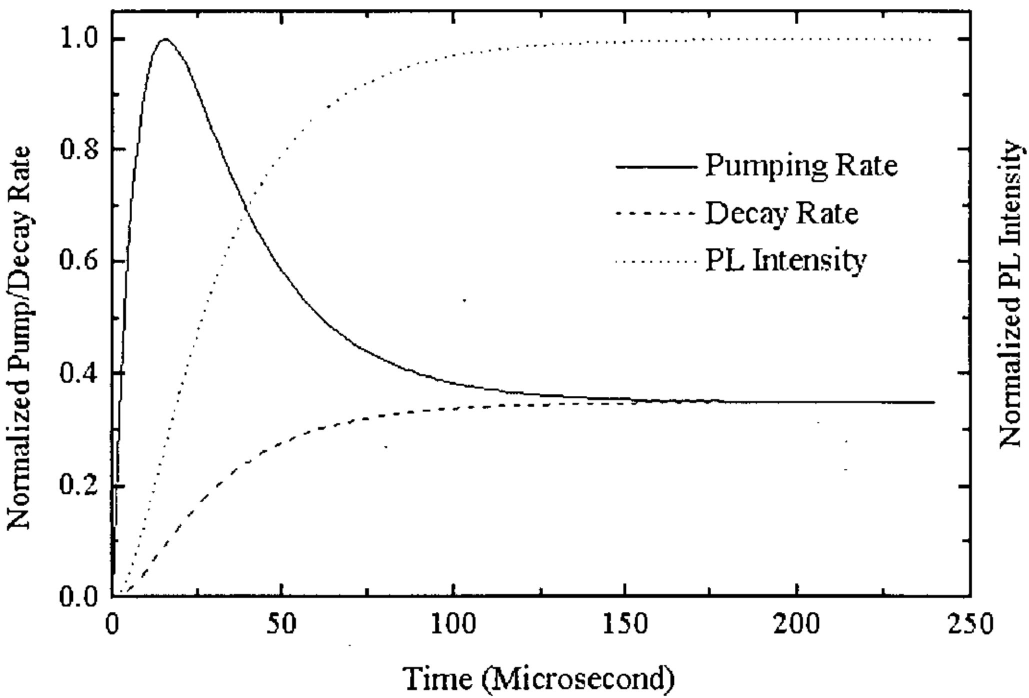

FIG. 5.10 Calculated PL intensity, pumping rate and decay rate profile under constant photo-excitation of 25 mW. $N_{er} = 3\times10^{17}$, $N_a = 1.5\times10^{16}$ per cm^3, T = 9 K and τ = 13 μs have been used.

Initially when large number of Er atoms are available for excitation the pumping rate is very high compared to decay rate. This causes a sharp initial increase in number of excited Er atoms and PL intensity. But as the number of excited Er atoms

increases the number of available Er atoms for excitation decreases. So pumping rate starts to decrease. Eventually the two rates become equal and PL intensity reaches steady state value.

Now let us see what happens when the excitation pulse is switched off before the PL intensity reaches steady state. The scenario is depicted in Figure 5.11. After the termination of laser pulse, excess carrier density starts to fall exponentially.

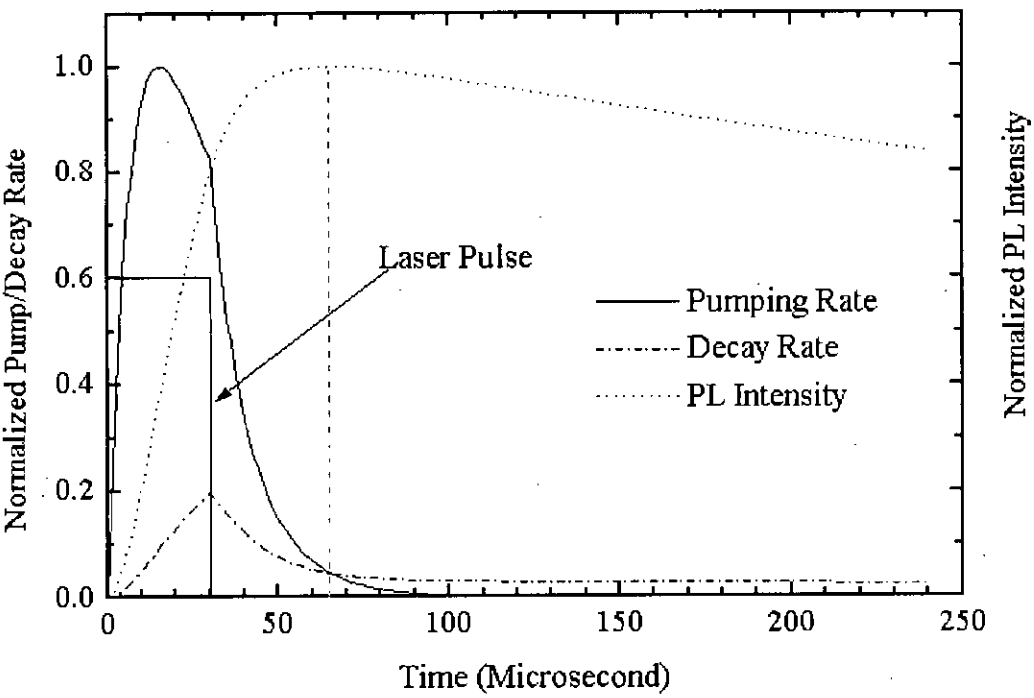

FIG. 5.11 Calculated PL intensity, pumping rate and decay rate profile for 30 μs laser pulse with an excitation of 25 mW. $N_{er} = 3\times10^{17}$, $N_a = 1.5\times10^{16}$ per cm^3, T = 9 K and $\tau = 13$ μs have been used.

But still for certain amount of time there are a large number of excess carriers which can provide sufficient pumping. So even after the termination of laser pulse of 30 μs the pumping rate is substantially larger than the decay rate. As long as pumping rate is higher, PL intensity continues to rise. When pumping rate is equal to decay rate the intensity is maximum which is indicated by light dashed line in the figure. After that pumping rate becomes smaller than decay rate and PL intensity starts to fall.

Figure 5.12 shows calculated data and experimental data on the same plot. The experimental data was extracted from Shin et al. [17]. Same experimental conditions have been used in our calculation with one assumtion. Nothing is stated about the spot diameter of the laser used in the experiment. We used a laser spot

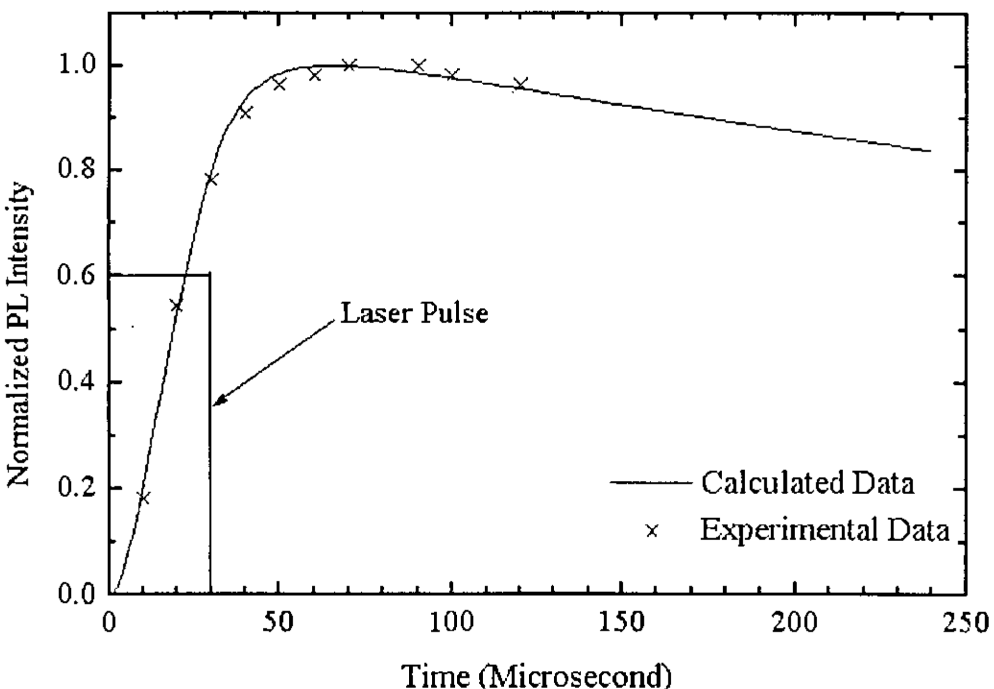

FIG. 5.12 Calculated PL intensity profile under 30 μs laser pulse excitation of 100 mW. $N_{er} = 3\times10^{17}$, $N_a = 1.5\times10^{16}$ per cm^3, T = 9 K and τ = 13 μs have been used. Excellent match with experimental data extracted from Shin et al. [17] has been found.

diameter of 6 mm with 1 μm penetration depth as used in other calculations. As seen in the figure, the calculated data fits well with the experimental data.

The extended rise effect of luminescence will certainly impose a serious limitation to achieving high-speed optoelectronic devices. If it is possible to minimize this effect then high-speed operation is possible. From our previous discussion it can be predicted that if we can manage to increase the decay rate of excited Er then problem related to this extended rise may be overcome.

One way of increasing the decay rate is by increasing temperature. In Figure 5.13 we have plotted luminescence profile for two different temperatures. With increasing temperature, the intensity will fall as shown previously. The two curves in the figure have been normalized to their peak intensities. It can be seen that by increasing temperature the effect of extended rise can definitely be minimized.

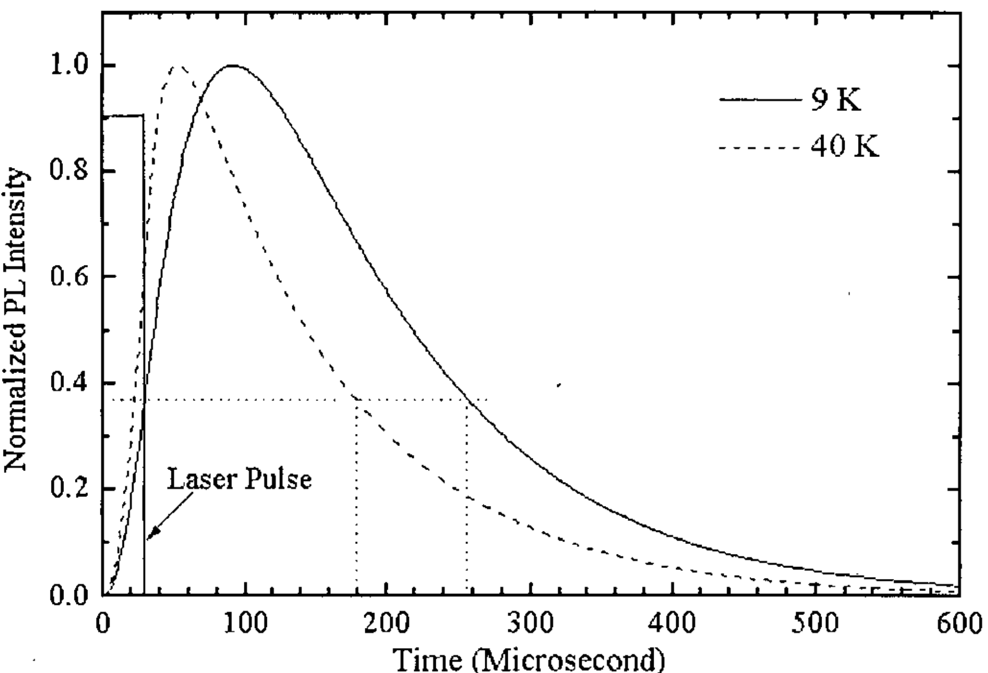

FIG. 5.13 Calculated PL intensity profile under 30 μs laser pulse excitation of 1 mW at two different temperatures. $N_{er} = 10^{17}$, $N_d = 4\times10^{17}$ per cm^3 have been used. $\tau = 40\ \mu s$ at T = 9 K and $\tau = 11.5\ \mu s$ at T = 40 K. Both the curves have been normalized to peak values.

If we define time constant as the time to reach 1/e or 36.8% of the peak value, the time constant for elevated temperature is much lower than that of the lower temperature case.

Another way of increasing decay rate is to increase excess carrier density by increasing excitation power. Figure 5.14 shows two PL profiles at two different excitation levels. Here also the curves have been plotted after normalizing to

respective peak intensities. For this case also we can see that the time constant for higher excitation power is lower than that for lower excitation power.

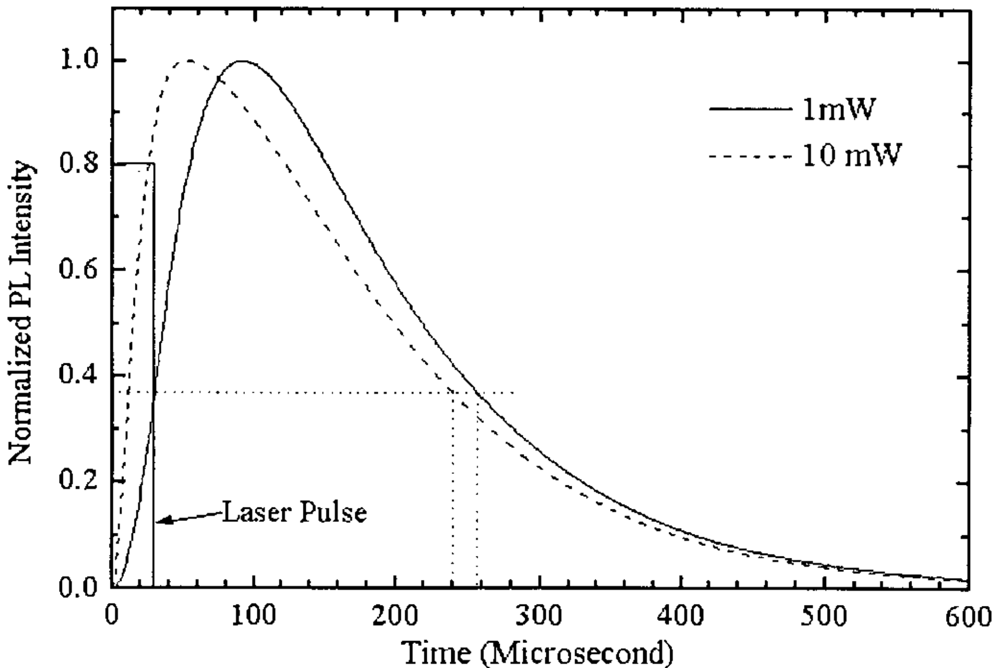

FIG. 5.14 Calculated PL intensity profile under 30 μs laser pulse excitation at two different excitation levels. $N_{er} = 10^{17}$, $N_d = 4\times10^{17}$ per cm^3, T = 9 K, τ = 40 μs have been used. Both the curves have been normalized to peak values.

At higher temperature PL intensity reduces drastically as shown in Figure 5.6. Using higher excitation, this problem may be eliminated. But, from the saturation of PL intensity shown in Figure 5.1 it can be said that increasing excitation to an arbitrarily high value may not improve the profile. A combination of appropriate temperature and excitation will yield the best result.

5.6 Stimulated emission and absorption

Now we shall investigate the possibility of obtaining laser from Er doped Si. In section 4.4 we have derived the expression of excited Er density taking into account both stimulated emission and absorption. The difference between density of atoms in excited state and unexcited state, $(N_2 - N_1)$ is plotted against excess carrier density

in Figure 5.15. Excess carriers in this case can be supplied by electrical excitation. It has been found that in n-type material it is not possible to achieve inversion using the values of different parameters used in our model. But in p-type Si it is possible to obtain inversion. Not only that, ($N_2 - N_1$) rises substantially with increasing excess carrier density and saturates at a particular level in p-type Si.

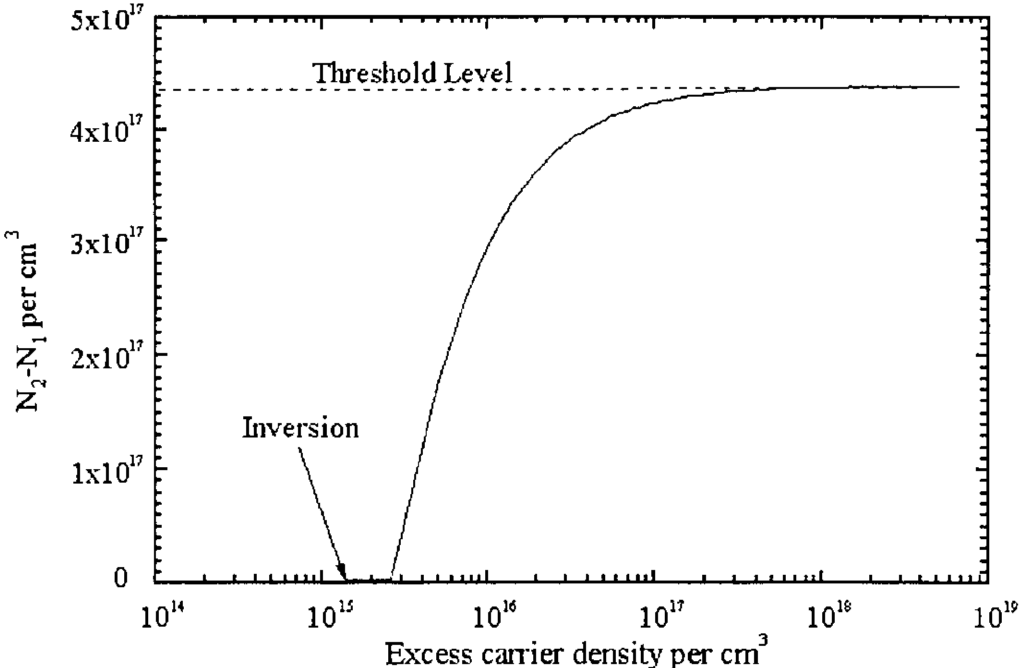

FIG. 5.15 Variation of N_2-N_1 with excess carriers with stimulated emission and absorption taken into consideration. $N_{er} = 10^{18}$, $N_a = 4\times10^{16}$ per cm^3, T = 4.2 K, $\tau = 5.8$ μs have been used.

Now we need to find out if it is possible to achieve threshold in p-type material. In order to find out the value of ($N_2 - N_1$) required at threshold, i.e., N_{th} , the values of following parameters are taken from Xie et al. [13]

loss coefficient $\gamma = 5$ cm^{-1},

reflectance of the mirrors used in cavity $R_1 = R_2 = 90\%$.

Values of other parameters used for calculation are

cavity length L = 300 μm,

thickness of Er doped region $L_{er} = 1$ μm,

free-space wavelength $\lambda = 1.54$ μm,

$\Delta\lambda$ corresponding to $\Delta\nu$ = 1.32 nm,

refractive index of Si for 1.54 μm wavelength = 3.46

Though the values used in [13] are said to be overly optimistic, we have found out that the value of N_{th} required is 4.3532×10^{17} per cm^3 which is marked by dashed line in Figure 5.15. From figure 5.15 we can see that $(N_2 - N_1)$ saturates at a value slightly greater than this value. So we can conclude that in a overly optimistic case it is possible to construct a laser device using p-type Er doped Si.

Now let us see if the laser device we proposed in section 4.6 is capable of supplying laser power. We will start our analysis from threshold condition, as below threshold there will be no output from laser device. The concentration of excited Er atoms, N_2 and that of unexcited Er atoms, N_1 at threshold have been calculated from values of Er density and N_{th}. Above threshold N_1 and N_2 will remain constant, as the laser system must reach steady state condition. Ignoring ρ_ν below threshold we have calculated the value of excess carrier density at threshold, n_{thrs} using equation (4.5.1) and then calculated corresponding current density using equation (4.6.2.3). We have marked this value of current density as J_{thrs} . Starting from n_{thrs} we have increased the value of injected excess carrier density and using the equations presented in sections 4.5 and 4.6.2, calculated the corresponding values of power density, ρ_ν and current density, J. Then we plotted ρ_ν vs. J. Figure 5.16 shows the resulting curve. We have chosen ρ_ν as y-axis variable as this is directly proportional to output power. We can see that the output power increases linearly with injected current density which is typical to most other semiconductor lasers. Though it was not possible for us to calculate the exact numerical value of output power for a particular injection level, we can conclude that our proposed laser device is capable of producing output power as the injection current exceeds a threshold value.

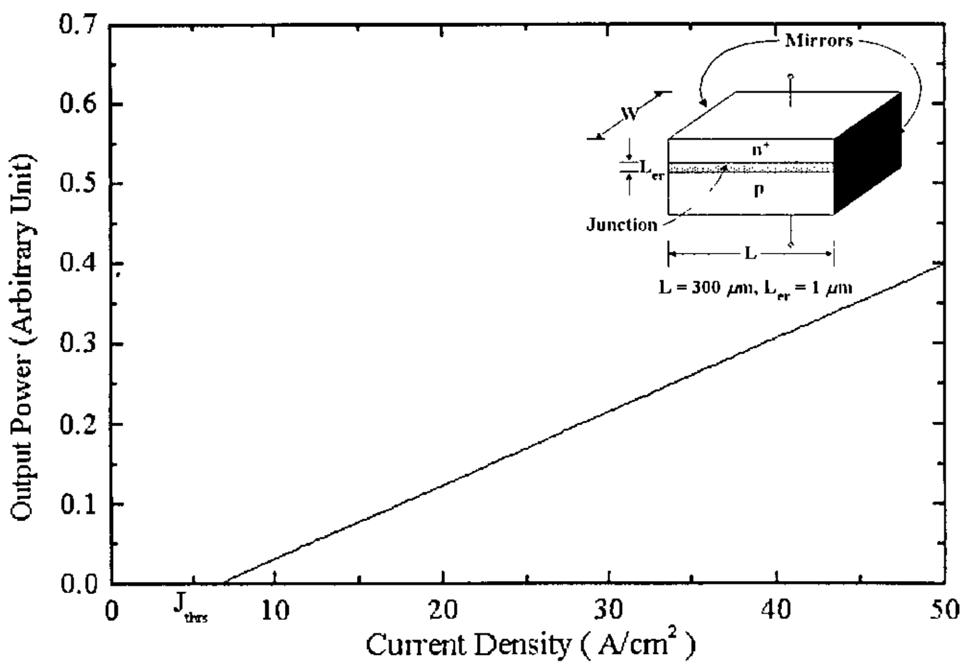

FIG. 5.16 Calculated output power dependence of semiconductor laser on injected current density. $N_{er} = 10^{18}$, $N_a = 4\times10^{16}$ per cm^3, T = 4.2 K, τ = 5.8 μs have been used.

Chapter 6

Conclusion

Er doped Si offers enormous potential for fabrication of optoelectronic devices on Si wafers using conventional fabrication technology. In this thesis, the optical properties of Er have been discussed. The excitation mechanism of Er in Si has been explained using Shockley-Read-Hall recombination kinetics. Using SRH recombination kinetics, a mathematical model for both spontaneous and stimulated excitation of Er in both p-type and n-type Si has been proposed. The model has been designed to incorporate high excitation levels and typical room temperature effects. Good agreement with experimentally obtained results has been achieved. The sharp quenching of Er luminescence with temperature has been explained. Also, effects of doping, excitation power etc. on Er luminescence have been explained. The unusual effect of extended rise of Er luminescence under short excitation pulse has been explained mathematically. Some suggestions have been made regarding the possible high-speed operation of Er doped Si devices.

The possibility of obtaining laser from EDS has been investigated and a laser device has been proposed. An estimation of the output power of the proposed laser device has been made. It has been found that the output power of the laser device increases linearly with injection current above threshold.

6.1 Recommendation for future work

Practical use of Erbium luminescence is yet to be achieved due to strong quenching of the luminescence at room temperature. Introduction of co-dopants like Oxygen has been found to reduce the temperature quenching mechanism significantly. Also operating in reverse biased condition enhances the high temperature luminescence.

Yet more research on reduction of luminescence quenching at higher temperature is to be carried out in order to fabricate Si:Er optoelectronic devices operating at room temperature. The field of research may be directed to impurity enhancement of luminescence.

The extended rise of luminescence under short excitation pulse imposes serious limitation on the possible high speed operation of Si:Er optoelectronic systems. Though in section 5.5 we have proposed a way to reduce the effect, more research may be carried out in this field.

As shown by experiments, Er doping and background concentration have significant influence on the luminescence intensity. Concentration of Er in Si is determined by the solid solubility limit. Even if Si is doped with highest possible Er concentration, not all Er atoms become electrically or optically active. Co-dopants has been found to increase the electrical and optical activation of Er atoms in Si. So optimum concentrations of Er, co-dopant and donor(or acceptor) are to be determined for the most efficient operation of Si:Er devices.

In our research we have performed only a theoretical analysis on possible attainment of laser from Er doped Si. According to our analysis, it is possible to construct laser device from Er doped p-type Si. However, there remains a scope of extensive research in this field. Detailed study of the pumping process, loss mechanisms, conditions for population inversion etc. is necessary for the implementation of a prospective Silicon laser. In our analysis we have assumed that beam remains totally confined within the Er doped region which is not practical. Study of $Si_{1-x}Ge_x$/Si:Er systems for good optical as well as electrical confinement may be carried out. Modulation techniques for laser and LEDs may be another topic of research. Comparative study between laser and LED in integrated system design may be made. Transmission and detection of optical signal is essential in optoelectronic systems. So Si based waveguide and detectors may be another field of research.

Bibliography

[1] J. Michel, J. L. Benton, R. F. Farante, D. C Jacobson, D. J. Eaglesham, E. A. Fitzerald, Y. H. Xie, J. M. Poate, and L. C. Kimerling, "Impurity enhancement of the 1.54 μm Er^{3+} luminescence in silicon," *J. Appl. Phys.*, Vol. 70, p. 2672, 1991.

[2] G. Franzò, F. Priolo, S. Coffa, A. Polman, and A. Carnera, "Room-temperature electroluminescence from Er-doped crystalline Si," *Appl. Phys. Lett.*, Vol. 64, p. 2235, 1994.

[3] M. Q. Huda, S. A. Siddiqui, and M. S. Islam, "Explaining the erbium luminescence profile in silicon under short excitation pulses", *Solid State Communications*, Vol. 118, p. 235, 2001.

[4] L. T. Canham, W. Y. Leong, M. I. J. Beale, T. J. Cox, and L. Taylor, "Silicon quantum wire array fabrication by electrochemical and chemical dissolution of wafers," *Appl. Phys. Lett.*, Vol. 57, p. 1046, 1990.

[5] L. Tsybeskov, K. L. Moore, D. G. Hall, and P. M. Fauchet, "Intrinsic band-edge photoluminescence from silicon clusters at room temperature," *Phys. Rev. B*, Vol. 54, p. R8361, 1996.

[6] S. Fukatsu, N. Usami, Y. Shiraki, A. Nishida, and K. Nakagawa, "High-temperature operation of strained $Si_{0.65}Ge_{0.35}$/Si(111) *p*-type multiple-quantum-well light-emitting diode grown by solid source Si molecular-beam epitaxy," *Appl. Phys. Lett.*, Vol. 63, p. 967, 1993.

[7] L. T. Canham, K. G. Barraclough, and D. J. Robbins, "1.3-μm light-emitting diode from silicon electron irradiated at its damage threshold," *Appl. Phys. Lett.*, Vol. 51, p. 1509, 1987.

[8] H. Ennen, J. Schneider, G. Pomrenke, and A. Axmann, "1.54-μm luminescence of erbium-implanted III-V semiconductors and silicon," *Appl. Phys. Lett.*, Vol. 43, p. 943, 1983.

[9] *Rare earth doped semiconductors*, edited by G. S. Pomrenke, P. B. Klein, D. W. Langer, MRS Symp. Proc No. 301, Materials Research Society, Pittsburgh, 1993.

[10] *Rare earth doped semiconductors II*, S. Coffa, A. Polman, R. N. Schwartz, MRS Symp. Proc No. 422, Materials Research Society, Pittsburgh, 1996.

[11] K. N. R. Taylor and M. I. Darby, *Physics of rare earth solids*, Chapman and Hall, London, 1972.

[12] S. Hufner, *Optical spectra of transparent rare earth compounds*, Academic, New York, 1978.

[13] Y. H. Xie, E. A. Fitzgerald, and Y. J. Mii, "Evaluation of erbium-doped silicon for optoelectronic applications," *J. Appl. Phys.*, Vol. 70, p. 3223, 1991.

[14] S. Libertino, S. Coffa, G. Franzò, and F. Priolo, "The effects of oxygen and defects on the deep level properties of Er in crystalline Si," *Appl. Phys. Lett.*, Vol. 78, p. 3867, 1995.

[15] F. Priolo, G. Franzò, S. Coffa, A. Polman, S. Libertino, R. Barklie, and D. Carey, "The erbium-impurity interaction and its effect on the 1.54 μm luminescence of Er^{3+} in crystalline silicon," *Appl. Phys. Lett.*, Vol. 78, p. 3874, 1995.

[16] Francesco Priolo, Giorgia Franzò, Salvatore Coffa, and Alberto Carnera, "Excitation and nonradiative deexcitation processes of Er^{3+} in crystalline Si," *Phys. Rev. B*, Vol. 57, p. 4443, 1998.

[17] Jung H. Shin, G. N. van den Hoven, and A. Polman, "Direct experimental evidence for trap-state mediated excitation of Er^{3+} in silicon," *Appl. Phys. Lett.*, Vol. 67, p. 377, 1995.

[18] D.T.X. Thao, C.A.J. Ammerlaan, and T. Gregorkiewicz, "Photoluminescence of erbium-doped silicon: Excitation power and temperature dependence," *J. Appl. Phys.*, Vol. 88, p. 1443, 2000.

[19] J. Palm, F. Gan, B. Zheng, J. Michel, and L. C. Kimerling, "Electroluminescence of erbium-doped silicon," *Phys. Rev. B*, Vol. 54, p. 17603, 1996.

[20] S. Coffa, F. Priolo, G. Franzò, A. Carnera, and C. Spinella, "Optical activation and excitation mechanism of Er implanted in Si," *Phys. Rev. B*, Vol. 48, p. 11782, 1993.

[21] P. G. Kik, M. J. A. de Dood, K. Kikoin, and A. Polman, "Excitation and deexcitation of Er^{3+} in crystalline silicon," *Appl. Phys. Lett.*, Vol. 70, p. 1721, 1997.

[22] Shun Lien Chuang, *Physics of optoelectronics devices*, Second edition, John Willy & Sons, New York, 1995.

[23] H. Ennen, J. Wagner, H. D. Müller, and R. S. Smith, "Photoluminescence excitation measurements on GaAs:Er grown by molecular-beam epitaxy," *J. Appl. Phys.*, Vol. 61, p. 4877, 1987.

[24] Y. S. Tang, K. C. Heasman, W. P. Gillin, and B. J. Sealy, "Characteristics of rare-earth element erbium implanted in silicon," *Appl. Phys. Lett.*, Vol. 55, p. 432, 1989.

[25] D. L. Alder, D. C. Jacobson, D. J. Eaglesham, M. A. Marcus, J. L. Benton, J. M. Poate, and P. H. Citrin, "Local structure of 1.54-μm-luminescence Er^{3+} implanted in Si," *Appl. Phys. Lett.*, Vol. 61, p. 2181, 1992.

[26] J. L. Benton, J. Michel, L. C. Kimerling, D. C. Jacobson, Y. H. Xie, D. J. Eaglesham, E. A. Fitzgerald, and J. M. Poate, "The electrical and defect properties of erbium-implanted silicon," *J. Appl. Phys.*, Vol. 70, p. 2667, 1991.

[27] F. Priolo, S. Coffa, G. Franzò, C. Spinella, A. Carnera, and V. Bellani, "Electrical and optical characterization of Er-implanted Si : The role of impurities and defects," *J. Appl. Phys.*, Vol. 74, p. 4936, 1993.

[28] S. Coffa, G. Franzò, F. Priolo, A. Polman, and R. Serna, "Temperature dependence and quenching processes of the intra-4f luminescence of Er in crystalline Si," *Phys. Rev. B*, Vol. 49, p. 16313, 1993.

[29] G. Franzò, S. Coffa, F. Priolo, and C. Spinella, "Mechanism and performance of forward and reverse bias electroluminescence at 1.54 μm from Er-doped Si diodes," *J. Appl. Phys.*, Vol. 81, p. 2784, 1997.

[30] S. Coffa, G. Franzò, and F. Priolo, "High efficiency and fast modulation of Er-doped light emitting Si diodes," *Appl. Phys. Lett.*, Vol. 69, p. 2077, 1996.

[31] J. Wilson and J. F. B. Hawkes, *Optoelectronics An Introduction*, Second edition, Prentice-Hall International (UK) Limited, 1996.

[32] Ben. G. Streetman, *Solid State Electronic Devices*, Third edition, Prentice-Hall of India, p. 76, 1993.

[33] M. Q. Huda, A. R. Peaker, J. H. Evans Freeman, D. C. Houghton, and W. P. Gillin, "Strong luminescence from Erbium in $Si/Si_{1-x}Ge_x/Si$ quantum well structures," *Electronics Letters*, Vol. 33, p. 1182, 1997.

Appendix A

Flowchart for calculation of PL decay profile of Erbium in Silicon

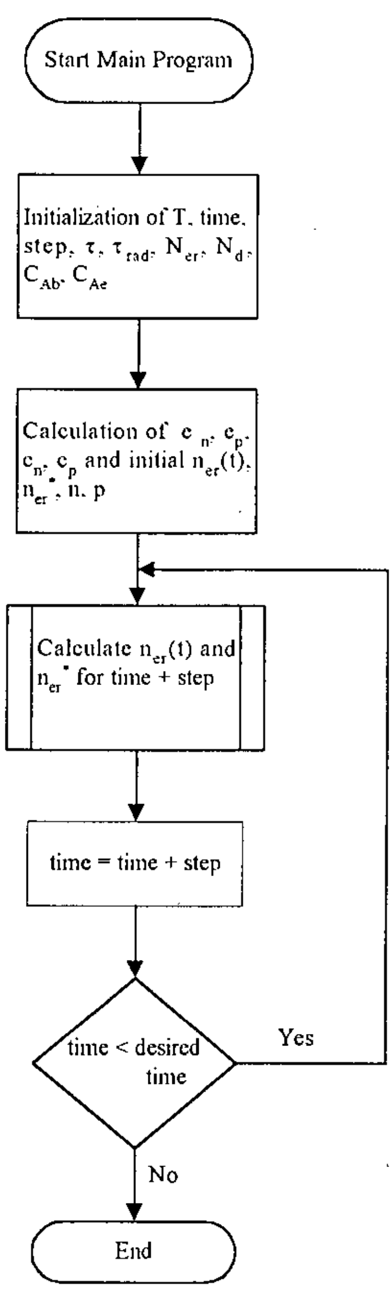

Appendix B

Expression for excited Erbium atoms considering stimulated emission and absorption

N_{er} = total number of active Er sites per unit volume

n_{er} = total number of active Er sites filled by electrons at a steady state of excitation per unit volume

n^*_{er} = total number of excited Er atoms at steady state per unit volume

f_t = fraction of Er sites occupied by electron, $\frac{n_{er}}{N_{er}}$

τ_{eq} = total decay lifetime of excited Er atoms

τ_{rad} = radiative lifetime of excited Er atoms

n = free electron concentration

p = free hole concentration

ρ_v = energy density, $N h\nu$

N = number of photons per unit volume having frequency ν.

Excitation rate of Er = $f_t c_p p(N_{er} - n^*_{er}) + (N_{er} - n^*_{er})\rho_v B_{12}$

and de-excitation rate = $\frac{n^*_{er}}{\tau_{eq}} + n^*_{er}\rho_v B_{21}$.

At steady state these two rates must be equal. So

$$f_t c_p p(N_{er} - n^*_{er}) + (N_{er} - n^*_{er})\rho_v B_{12} = \frac{n^*_{er}}{\tau_{eq}} + n^*_{er}\rho_v B_{21}$$

Now the photon generation rate and decay rate can be equated at steady state. Hence

$$(N_{er} - n^*_{er})\rho_v B_{12} = \frac{n^*_{er}}{\tau_{rad}} + n^*_{er}\rho_v B_{21}$$

If $B_{12} = B_{21}$ then we get

$$\rho_v B_{21} = \frac{n_{er}^*}{\tau_{rad}(N_{er} - 2n_{er}^*)}$$

So the rate equation of excited Er atoms becomes

$$f_t c_p p(N_{er} - n_{er}^*) + \frac{n_{er}^*(N_{er} - n_{er}^*)}{\tau_{rad}(N_{er} - 2n_{er}^*)} = \frac{n_{er}^*}{\tau_{eq}} + \frac{n_{er}^{*2}}{\tau_{rad}(N_{er} - 2n_{er}^*)}$$

Multiplying both sides by $\tau_{eq}\tau_{rad}(N_{er} - 2n_{er}^*)$

$$f_t c_p p \tau_{rad}\tau_{eq}(N_{er} - n_{er}^*)(N_{er} - 2n_{er}^*) + n_{er}^*\tau_{eq}(N_{er} - n_{er}^*) = n_{er}^*\tau_{rad}(N_{er} - 2n_{er}^*) + n_{er}^{*2}\tau_{eq}$$

putting $S = f_t c_p p \tau_{rad}\tau_{eq}$

$$S\left(N_{er}^2 - 3N_{er}n_{er}^* + 2n_{er}^{*2}\right) + N_{er}n_{er}^*\tau_{eq} - n_{er}^{*2}\tau_{eq} = N_{er}n_{er}^*\tau_{rad} - 2n_{er}^{*2}\tau_{rad} + n_{er}^{*2}\tau_{eq}$$

$$\Rightarrow 2(\tau_{rad} - \tau_{eq} + S)n_{er}^{*2} + (\tau_{eq} - \tau_{rad} - 3S)N_{er}n_{er}^* + SN_{er}^2 = 0$$

$$\Rightarrow 2(\tau_{rad} - \tau_{eq} + S)n_{er}^{*2} - (\tau_{rad} - \tau_{eq} + S)N_{er}n_{er}^* - 2SN_{er}n_{er}^* + SN_{er}^2 = 0$$

$$\Rightarrow n_{er}^*(\tau_{rad} - \tau_{eq} + S)(2n_{er}^* - N_{er}) - SN_{er}(2n_{er}^* - N_{er}) = 0$$

$$\Rightarrow (2n_{er}^* - N_{er})\left\{n_{er}^*(\tau_{rad} - \tau_{eq} + S) - SN_{er}\right\} = 0$$

So $\quad 2n_{er}^* - N_{er} = 0 \quad$ or $\quad n_{er}^*(\tau_{rad} - \tau_{eq} + S) - SN_{er} = 0$

That means

$$n_{er}^* = \frac{N_{er}}{2} \quad \text{or} \quad n_{er}^* = \frac{S}{\tau_{rad} - \tau_{eq} + S}N_{er}$$

But $n_{er}^* = \frac{N_{er}}{2}$ is not acceptable as this means n_{er}^* is a constant quantity for a particular Er doping level and does not depend on excitation, i.e., input power. So

$$n_{er}^* = \frac{S}{\tau_{rad} - \tau_{eq} + S}N_{er}$$

Putting the value of S

$$n_{er}^* = \frac{f_t c_p p \tau_{rad}\tau_{eq}}{\tau_{rad} - \tau_{eq} + f_t c_p p \tau_{rad}\tau_{eq}}N_{er} = \frac{f_t c_p p}{f_t c_p p + \frac{1}{\tau_{eq}} - \frac{1}{\tau_{rad}}}N_{er}$$

রাজশাহী বিশ্ববিদ্যালয় গ্রন্থাগার
নং 25948
27.1.02